UNIVERSITY OF CALIFORNIA SAN DIEGO

Bridging the Gap: Insights into the eIF4E-eIF4G1-PABP1-mRNA Complex

A Thesis submitted in partial satisfaction of the requirements for the degree

Master of Science

in

Chemistry

by

Alberto Pequeno

Committee in charge:

Simpson Joseph, Chair
Gourisankar Ghosh
Jeremy Klosterman

2018

The Thesis of Alberto Pequeno is approved, and it is acceptable in quality and form for publication on microfilm and electronically:

_____

_____

_____

Chair

University of California San Diego

2018

TABLE OF CONTENTS

LIST OF FIGURES

ACKNOWLEDGEMENTS

I am very grateful for the opportunity given to me by Professor Simpson Joseph. Though I did not have any prior research experience, he welcomed me into his lab and provided me with the tools and guidance to succeed. He has been an excellent mentor during these past two years.

I would also like to thank every member of the Joseph lab. Everyone has been extremely helpful to me in one way or another. I could not have learned everything that I have without their help.

Finally, I would like to thank all my family for their continued prayers and support. I am especially thankful for my wife Becky. During the toughest days, she would be there to cheer me up and help keep me motivated. During the best days, she would be there to share my excitement.

ABSTRACT OF THE THESIS

Bridging the Gap: Insights into the eIF4E-eIF4G1-PABP1-mRNA Complex

by

Alberto Pequeno

Master of Science in Chemistry

University of California San Diego, 2018

Professor Simpson Joseph, Chair

Translation initiation is a highly regulated process that plays a significant role in maintaining homeostasis. It has been shown to be a critical step in the proliferation of cancer and a crucial target for a variety of viruses. Thus, it has become an attractive target for the development of therapeutic drugs. Further knowledge of the mechanism of translation initiation might be beneficial in improving the efficiency of novel therapeutic drugs.

Though extensive work has been done to understand the mechanism in different species, studies of human translation initiation (specifically the eIF4E ●

eIF4G1 ● PABP1 interactions) have been limited to cell-based assays and the use of small recombinant eIF4G1 variants.

Here we use a recombinant variant of eIF4G1 capable of interacting with both eIF4E and PABP1 to determine possible complex formations in the presence of different mRNAs. We find that complex formation is possible with a variety of mRNAs and in the presence or absence of the m^7G cap or poly A tail. Furthermore, we demonstrate that eIF4G1 modulates eIF4E cap binding affinity and preferentially interacts with cap-bound eIF4E using a previously unidentified region. Finally, we show that eIF4G1 possess an additional RNA binding domain in its N-terminal region.

Chapter 1: Introduction

1.1 Background

Proteins are complex macromolecules that are responsible for a large array of cellular functions. Some of their functions include, but are not limited to, serving as antibodies to help protect the body from foreign invaders, enzymes for chemical reactions, messengers, structural components, and transport. Given its multitude of functions, it is evident that proteins are a critical component for the well-being and survival of an organism.

Genetic information is transferred from DNA to mRNA through a process called transcription, then to proteins through translation. Protein synthesis (translation) in eukaryotes is a complex process that involves a multitude of factors and is divided into three key steps: (1) initiation, (2) elongation, (3) termination. Misregulation of translation can lead to detrimental effects such as cancer[1-4]. Furthermore, the translation machinery has been shown to be a crucial target for a variety of viruses[5-12]. For these reasons, translation initiation has become an attractive therapeutic target for novel drugs[13-17].

1.2 Translation Initiation

Eukaryotic translation initiation has been characterized as a highly regulated and rate-limiting step for protein synthesis[18]. Canonical translation initiation begins with a 5' – 7- methylguanosine capped (m^7G cap) and 3' polyadenylated (poly(A) tail) messenger RNA (mRNA). Various proteins, which includes a group of eukaryotic translation initiation factors (eIFs), play a significant role in the "activation" of the mRNA and the recruitment of the ribosome. The m^7G cap and poly (A) tail are recognized and bound by eIF4E and polyadenylate-binding protein 1 (PABP1), respectively. A stable "closed loop" messenger ribonucleoprotein (mRNP) structure is formed by the interactions of eIF4E, PABP1, and mRNA with eIF4G1 (Figure 1.1). The helicase protein eIF4A1, which also binds directly to eIF4G1, is recruited along with its accessory protein eIF4B to break secondary mRNA structures. The 43S preinitiation complex (PIC) consists of the 40S ribosomal subunit ,eIF1, eIF1A, eIF3, eIF5, GTP bound eIF2, and a initiator methionyl-tRNA (Met-$tRNA_i$) (Figure 1.1). The 43S PIC is then bridged to the "activated" mRNA through eIF3's interaction with eIF4G1. This positions the 43S PIC near the m^7G cap which allows for mRNA scanning and recognition of the AUG start codon. Start codon recognition caused by Met-$tRNA_i$ base pairing induces the conversion of GTP-eIF2 to GDP-eIF2 and brings about the release of itself and several other eIFs. Lastly, incorporation of

the large 60S ribosomal subunit generates an 80S PIC which initiates the elongation phase of translation.

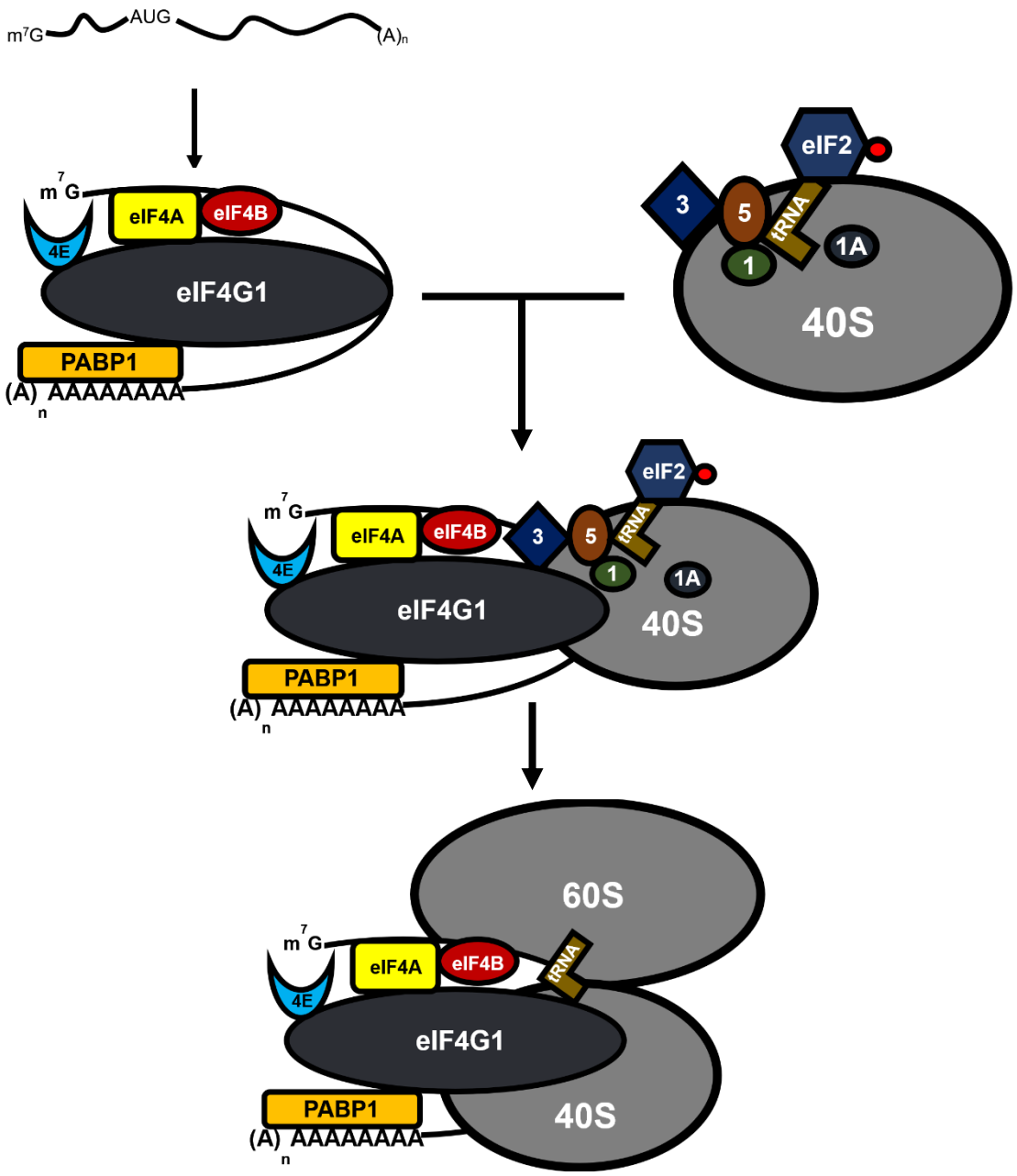

Figure 1.1: Eukaryotic translation initiation. A model depicting key steps of eukaryotic translation initiation. tRNA represents Met-tRNA$_i$. Light red circle represents GTP. eIF1 (green), eIF1A (black), eIF3 (dark blue), eIF5 (brown), and eIF4E (light blue) are labeled without the "eIF" in the diagram.

1.3 Architecture of eIF4E, eIF4G1, and PABP1

Human eIF4E is a 217 amino acid (~25 kDa) protein consisting of an N-terminal disordered region (aa 1-35), four α helices, and eight antiparallel β sheets which give it an overall "cupped hand" shape[19-23]. The 5' m^7G cap has been shown to sit between two tryptophan residues that reside in the concave region of eIF4E[19-23]. The binding affinity of eIF4E for the 5' m^7G cap has been reported as a broad range (100 – 450 nM) by different groups and has been shown to be dependent on salt concentration[24-26].

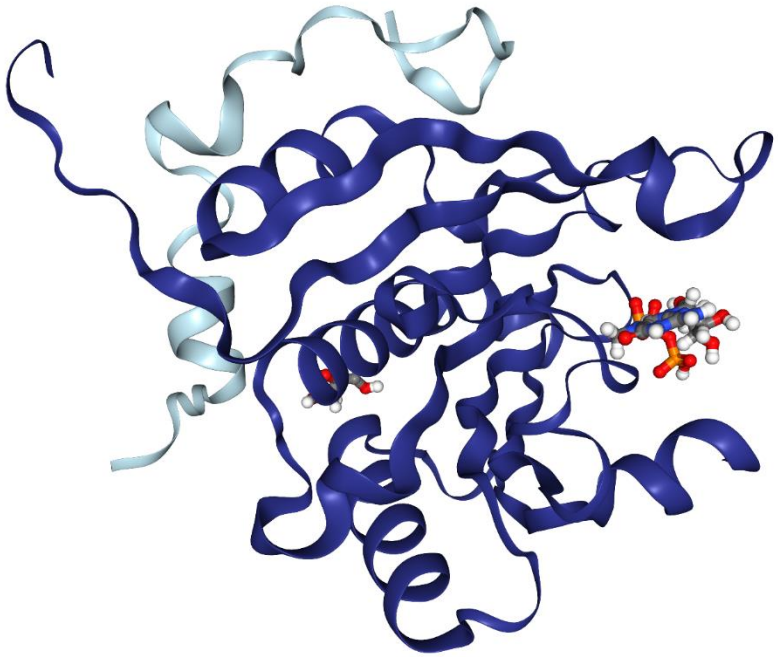

Figure 1.2: Crystal structure of the human eIF4E-eIF4G1 complex. Human eIF4E (indigo) bound to m^7GpppG cap analog and human eIF4G1 592-653 (light blue). Protein data code 5T46.

Human eIF4G1 is a 1599 amino acid (~176 kDa) protein that has been shown to possess numerous protein and RNA binding sites. This allows it to serve the bridge linking serval components of the translation initiation complex. The N-terminal region contains binding sites for PABP1 (a.a. 172-200) and eIF4E (a.a. 612-618; a.a. 632-642)[27-32]. In its middle region, eIF4G1 possesses two RNA-binding domains (a.a. 682-721, 773-115), along with binding sites for eIF3 and eIF4A[33-37]. The C-terminal region contains a separate eIF4A and an Mnk1 protein kinase binding site[35,37].

Figure 1.3: Architecture of human eIF4G1. The relative location of each domain is depicted above.

PABP1 is a 636 amino acid (~70 kDa) protein consisting of four N-terminal RNA recognition motifs (RRMs), a proline-rich linker, and a C-terminal domain[38-40]. PABP1 binds to poly A RNA through its RRMs with an affinity of ~ 4 nM[9,38,39,41,42]. Additionally, it binds to eIF4G1 cooperatively through RRM 2[29,30].

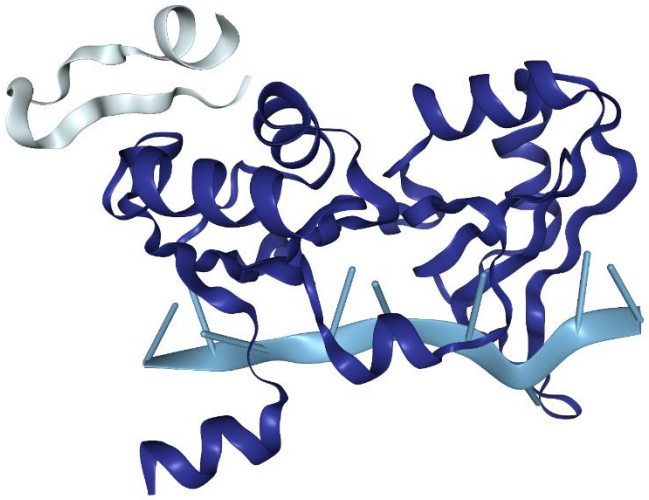

Figure 1.4: Crystal structure of the human PABP1 binding site of eIF4G1 in complex with RRM1-2 of PABP1 and poly(A). Human PABP1 RRM1-2 (indigo) bound to poly(A)$_{11}$ (blue) and human eIF4G1 161-216 (gray). Protein data code 4F02.

1.4 Significance of the m^{7}G cap, poly A tail, and their associated proteins

The role of the m^{7}G cap and poly A tail in translation initiation is one that cannot be belittled. Numerous studies have shown enhancement of translation efficiency as a result of a synergistic cooperation between the 5' m^{7}G cap, 3' poly A tail and their associated proteins[43-47]. Furthermore, disruption of these interactions has proven to be detrimental[40,45,48,49,54]. However, the synergy between the components allows for enhanced affinity and overall greater stability of the complex[50-54].

Several studies have shown that eIF4G1 is able to enhance the binding of eIF4E to the 5' m^{7}G cap through its direct association with the mRNA[33,51-53]. It is thought that eIF4G1 binds to mRNA through its middle region, thereby anchoring

the mRNA and enhancing the stability of the eIF4E ● m^7G cap complex. Similarly, it was shown that a small fragment of eIF4G1 was able to enhance the affinity of PABP1's RRM1-2 for poly A by 10-fold[30]. Additionally, immunoprecipitation experiments have shown an enhancement of cap bound eIF4E in the presence of eIF4G1 and PABP1[50]. Pull down experiments have also shown an enhanced eIF4G1 ● PABP1 interaction in the presence of eIF4E[39].

The role of the "closed-loop" messenger ribonucleoprotein structure in stimulating translation is quite interesting. Several mechanisms have been proposed to explain the functions of the "closed-loop" structure: (1) it promotes efficient ribosome recycling (2) it enhances the affinity and stability of the complex (3) it confirms the integrity of the mRNA (4) it stimulates the joining of the 60S ribosome[40,43-45,48,49]. With numerous interactions between components aiming to enhance its stability, it raises even more questions regarding its functions. Furthermore, the differences between species generates a greater interest in investigating the human complex.

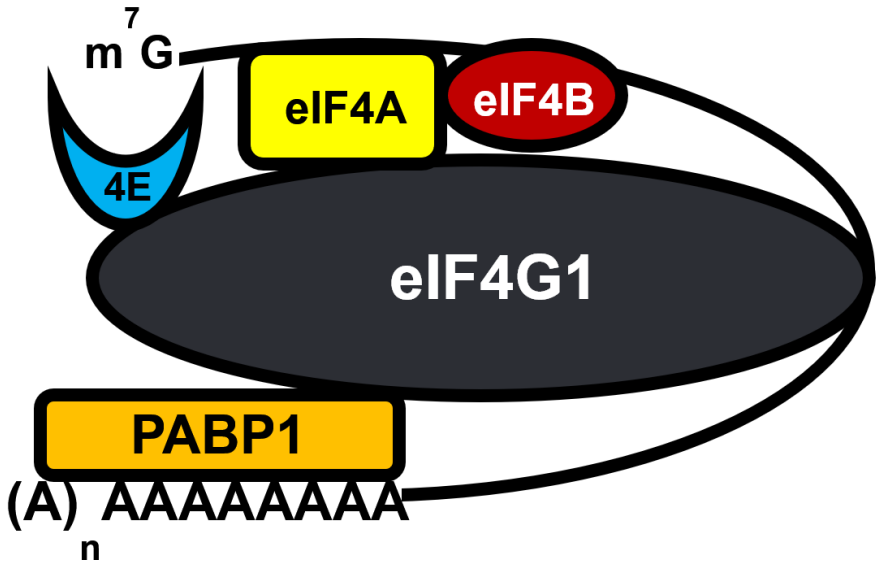

Figure 1.5: eIF4F ribonucleoprotein complex. Model of the “closed-loop” structure formed by eIF4E, eIF4G1, and PABP1 with m^7G capped and poly A-tailed mRNA.

Chapter 2: Expression and purification of human eIF4G1

2.1 Optimizing the purification of human eIF4G1 88-653

Previous studies have shown that recombinant expression and purification of human full length eIF4G1 is difficult. Thus, obtaining enough purified eIF4G1 for biochemical assays presents a challenge. Given our interest in studying the interactions between eIF4E, eIF4G1, and PABP1, we chose to isolate a region of eIF4G1 which binds to both eIF4E and PABP1 (Figure 2.1 A). The variant consisting of amino acids 88-653 was chosen for two reasons: (1) it contains both eIF4E and PABP binding sites (2) analysis using bioinformatics software (ExPASy) predicted this variant to have the highest stability of all the variants analyzed. The sequence coding for eIF4G1 88-653 was subcloned into various *E. coli* expression vectors containing different solubility fusion proteins and affinity tags. The expression vectors used were as follows: pMCSG7 (N-terminal hexahistidine tag), pMCSG9 (N-terminal hexahistidine tag and maltose binding protein (MBP) fusion), pMCSG10 (N-terminal hexahistidine tag and glutathione S-transferase (GST) fusion), pMCSG26 (C-terminal hexahistidine tag), and pETHSUL (N-terminal hexahistidine tag and small ubiquitin-like modifier (SUMO) fusion).

Each construct was tested for expression at various temperatures (37°C, 30°C, 25°C, 18°C, 12°C), isopropyl β-D-1-thiogalactopyranoside (IPTG)

concentrations (0.05 mM to 1 mM), OD600 (0.3 to 0.8), and length of induction (1, 2, 3, 4, 12, 16, 20 hrs.). Expression of recombinant eIF4G1 88-653 was poor regardless of vector or induction condition used. Purification of eIF4G1 88-653 was attempted using affinity chromatography with a variety of resins (Ni-NTA, amylose, glutathione sepharose) and buffer conditions (e.g. varying salt concentration, stabilization additives, denaturants, etc.). Nevertheless, efforts resulted in low yields and unsatisfactory purify of protein.

We sought to resolve our problem by enhancing protein expression through codon optimization. The sequence coding for eIF4G1 88-653 was codon optimized for *E. coli* expression (GENEWIZ), purchased as a FragmentGENE, and subcloned into the vectors mentioned above. Expression tests showed a significant improvement in recombinant eIF4G1 88-653 expression in all vectors. Unfortunately, purification attempts resulted in low yields and unsatisfactory purify yet again. This time however, the root of the problem stemmed from deficient binding to the affinity resin and not from poor expression. Various attempts to enhance binding to the resin (e.g. longer incubation times, increasing the amount of resin, using denaturants, etc.) proved to be unsuccessful. To attempt to circumvent the binding hindrance, a combination of ion exchange and size exclusion chromatography was employed. This method resulted in no significant improvement.

Finally, the sequence coding for eIF4G1 88-653 was subcloned into the pTXB1 vector (NEB) which contains a C-terminal Mxe GyrA Intein and a chitin

binding domain. This vector was chosen specifically due to the high affinity and specificity of the chitin binding domain for chitin resin. This method yielded a significant increase in recombinant (tagless) eIF4G1 88-653.

2.2 Isolation of additional eIF4G1 variants

Three additional eIF4G1 variants were purified from *E. coli* for our studies. The variant eIF4G1 190-653 is a 49 kDa protein that possesses a truncated PABP1 and complete eIF4E binding sites (Figure 2.1 C). To investigate the importance of the region between the PABP1 and eIF4E binding sites, we generated two variants which possess only one binding site. MBP-eIF4G1 69-214 is a 59 kDa maltose binding protein fusion protein that contains only the PABP1 binding site and flanking regions on both sides (Figure 2.1 D). MBP-eIF4G1 565-653 is a 54 kDa maltose binding protein fusion protein that contains only the eIF4E binding site and flanking regions on both sides (Figure 2.1 E). The MBP fusion was left on both constructs in order to mimic the size and isoelectric point (pI) of eIF4G1 88-653.

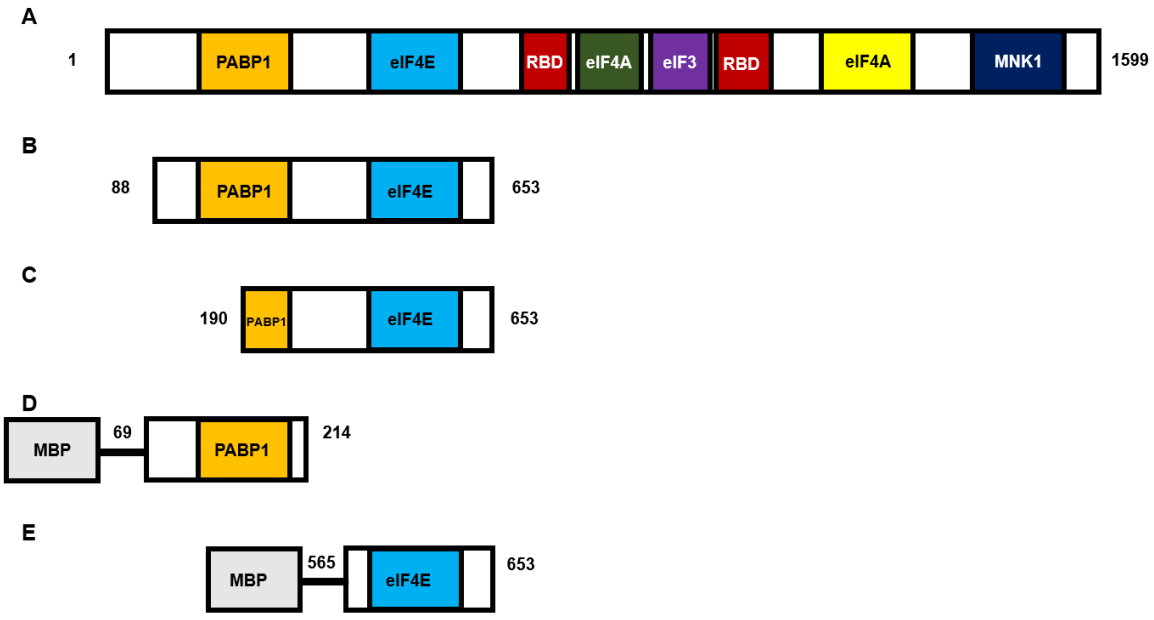

Figure 2.1: Architecture of human eIF4G1 variants. (A) Full length human eIF4G1 with known binding domains. (B-E) eIF4G1 variants used in this study. RBD is the RNA-binding domain.

Chapter 3: Investigating complex formation and interaction modulation between components

Introduction

The importance of the “closed-loop” messenger ribonucleoprotein structure formed by the interactions of eIF4E, PABP1, and mRNA with eIF4G1 is one that cannot be undervalued. Previous studies have shown that disruption of this complex dramatically impairs translation initiation[40,45]. Additionally, the synergistic cooperation between the 5’ m^7G cap and 3’ poly A tail to enhance translation initiation has been well documented in several species[43, 44, 46, 47]. In humans however, investigation of this complex has been limited to cell-based assays and biochemical studies using short fragments of eIF4G1.

In chapter 3 we use a large fragment of human eIF4G1 (containing both PABP1 and eIF4E binding sites), full length human eIF4E, and full length human PABP1 to perform qualitative and quantitative biochemical assays. Specifically, we test: (1) different complex formations using various mRNAs (Figure 3.1) (2) modulation of eIF4E cap binding affinity (3) eIF4E ● mRNA complex recognition by eIF4G1 and (4) RNA binding of eIF4G1. These assays provide insights into complex formation as well as how components modulate interactions between each other.

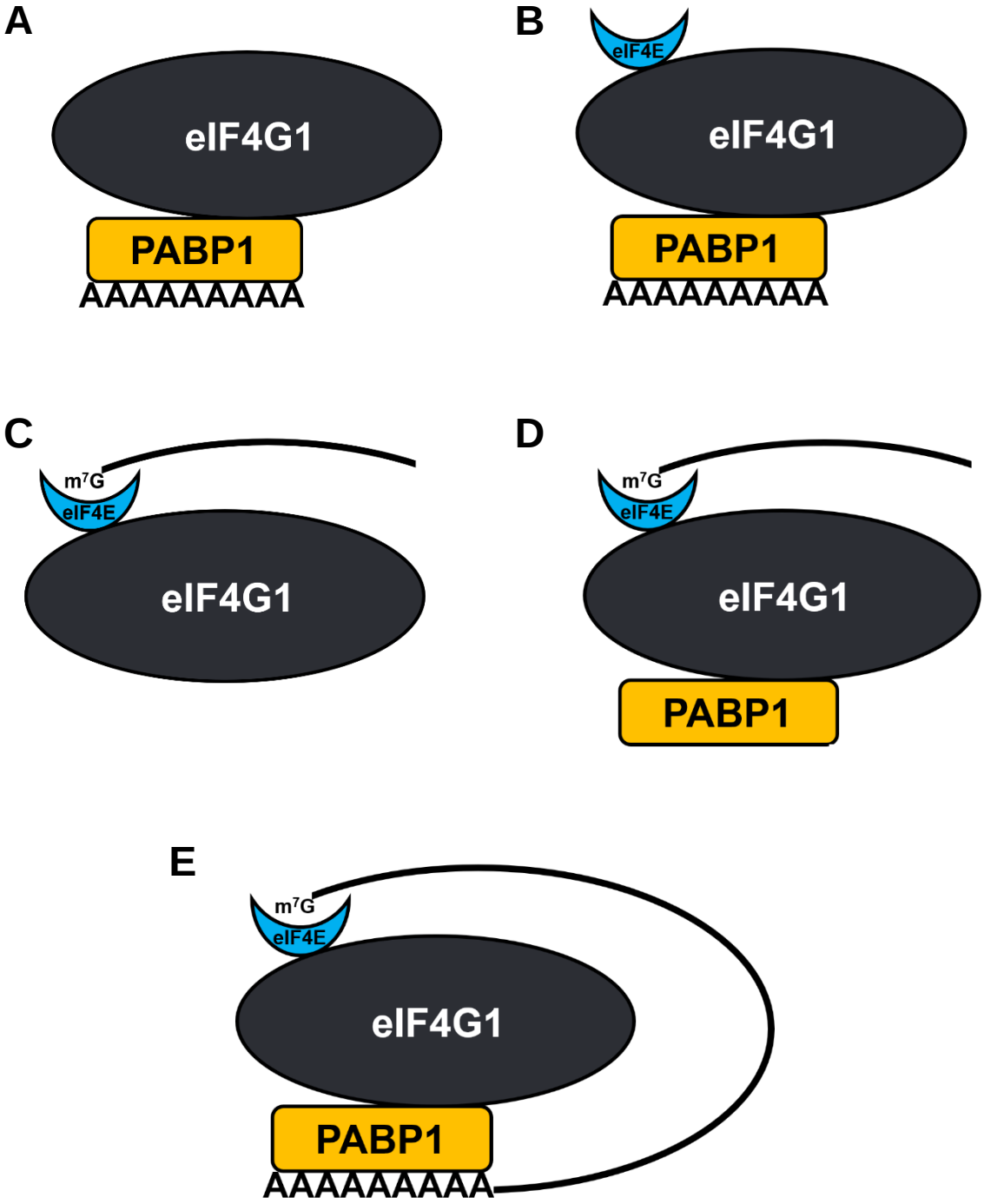

Figure 3.1: Ribonucleoprotein complexes. (A & B) complexes formed with Poly $A_{(18)}$ (C & D) complexes formed with m^7G capped mRNA but no poly A tail (E) "closed-loop" complex formed with m^7G capped and poly A tailed mRNA.

3.1 Poly A – PABP1 – eIF4G1 complex

To confirm that eIF4G1 88-653 was able to interact with full length PABP1, we used a gel shift assay with Poly $A_{(18)}$ RNA. Using a 5-fold excess of PABP1 to Poly $A_{(18)}$ RNA resulted in nearly a complete shift (Figure 3.2). This is consistent with the previously reported strong affinity of full length PABP1 for Poly A RNA[22, 23, 24]. To determine binding of eIF4G1 88-653 to the PABP1 ● Poly $A_{(18)}$ complex, eIF4G1 88-653 was titrated against a constant concentration of PABP1 and Poly $A_{(18)}$. Addition of eIF4G1 88-653 resulted in a concentration dependent super shift of Poly $A_{(18)}$ RNA (Figure 3.2). To rule out the possibility that the super shift was being caused by an interaction between eIF4G1 88-653 and Poly $A_{(18)}$, a control experiment was performed with just Poly $A_{(18)}$ and eIF4G1 88-653 (Figure 3.3, lane 3). Results show no interaction between the two, thus, indicating the formation of a Poly $A_{(18)}$ ● PABP1 ● eIF4G1 88-653 complex.

A previous study showed the affinity of eIF4G1 161-216 for a Poly $A_{(11)}$ bound RRM 1-2 PABP1 fragment to be in the micromolar range (K_D= 1.6 μM)[25]. Interestingly, in our study, the Poly $A_{(18)}$ ● PABP1 ● eIF4G1 88-653 complex seemed to form in the nanomolar range. The higher affinity of our complex could be due to a variety of reasons such as, using full length PABP1, a larger fragment of eIF4G1, or a combination of both. Further studies, such as repeating the gel shift assay with a smaller eIF4G1 fragment or solving the structure of the

Poly $A_{(18)}$ ● PABP1 ● eIF4G1 88-653 complex, could provide more insights and allow us to determine the reason(s) for the enhanced complex affinity.

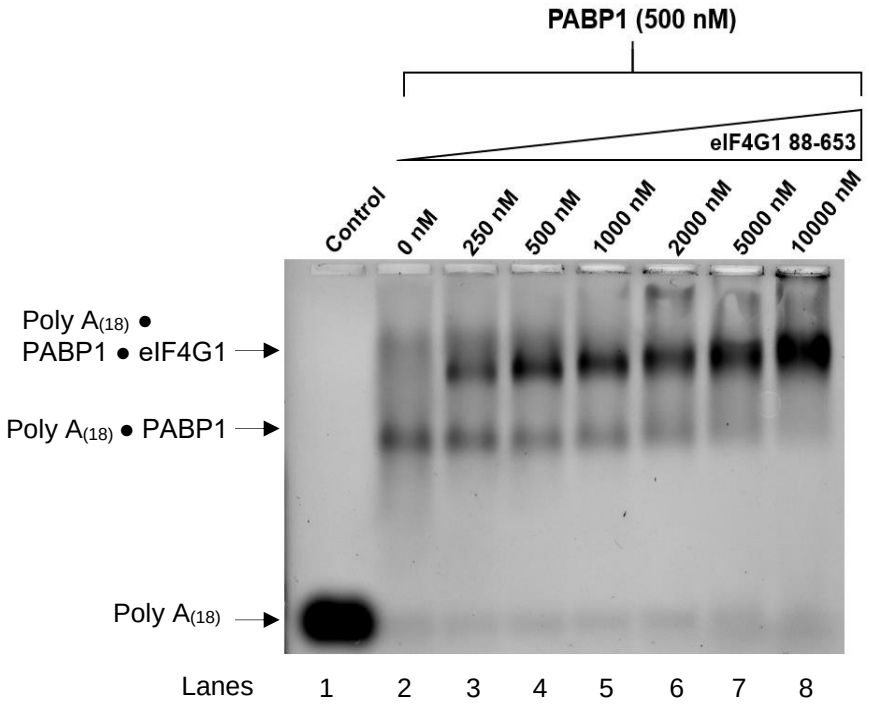

Figure 3.2: Gel shift assays of Poly $A_{(18)}$ ± PABP1 & eIF4G1. 0.7 % agarose gel. Binding of 100 nM Poly $A_{(18)}$ to 500 nM PABP1 with an increasing concentration of eIF4G1 88-653. RNA was 3' labeled with fluorescein.

3.2 Poly A – PABP1 – eIF4G1 – eIF4E complex

Having confirmed the formation of the Poly $A_{(18)}$ ● PABP1 ● eIF4G1 88-653 complex, we sought to determine if eIF4E would be able to form part of this complex without being bound to an m^7G cap. After verifying that eIF4E would not interact with Poly $A_{(18)}$, eIF4E was titrated against a constant concentration of PABP1, eIF4G1 88-653, and Poly $A_{(18)}$ (Figure 3.3). Without the addition of eIF4E, two distinct shifted bands which correspond to two different complexes can be seen: (1) Poly $A_{(18)}$ ● PABP1 and (2) Poly $A_{(18)}$ ● PABP1 ● eIF4G1 88-653. As the concentration of eIF4E increases, several differences can be observed: (1) there is a slight decrease in the intensity of the Poly $A_{(18)}$ ● PABP1 ● eIF4G1 88-653 band (2) there appears to be a slight shift of the Poly $A_{(18)}$ ● PABP1 band which becomes more apparent at higher eIF4E concentrations.

It is possible that the new slightly shifted band corresponds to a Poly $A_{(18)}$ ● PABP1 ● eIF4G1 88-653 ● eIF4E complex. While it would be expected for the larger complex to show even a greater shift than that of Poly $A_{(18)}$●PABP1● eIF4G1 88-653, several factors could account for the shift being less. It has been previously shown that conformational changes occur in both eIF4G1 and eIF4E upon binding[23,26,55,56]. Additionally, folding of eIF4G1 and PABP1 upon binding to each other and to Poly A have also been reported[30,39]. No extensive studies or structures have been reported for the complete PABP1 ● eIF4G1 ● eIF4E complex, thus it may be possible for additional conformational changes to occur

upon binding of all three proteins. If these conformational changes cause the complex to adopt a more compact structure, that could explain why the Poly $A_{(18)}$ ● PABP1 ● eIF4G1 88-653 ● eIF4E complex migrates farther down the gel than the Poly $A_{(18)}$ ● PABP1 ● eIF4G1 88-653 complex.

We then looked at how eIF4E might modulate the binding of eIF4G1 to the Poly $A_{(18)}$●PABP1. A previous study showed that PABP1 was able to pull down more eIF4G1 in the presence of eIF4E[39]. Interestingly, our gel shift assay (Figure 3.3) shows a very slight decrease in the Poly $A_{(18)}$ ● PABP1 ● eIF4G1 88-653 complex band with increasing eIF4E concentrations. Rather, the change is found in the Poly $A_{(18)}$●PABP1 band which seems to shift slightly at higher eIF4E concentrations. This begs the question: is the enhanced affinity of eIF4G1 for the Poly $A_{(18)}$ ● PABP1 complex a result of eIF4E binding to eIF4G1 first? This would suggest a mechanism in which eIF4E binds to eIF4G1 first before enhancing eIF4G1's affinity for the Poly A ● PABP1 complex. It would be interesting to see how this mechanism is affected in the presence of a full-length capped mRNA.

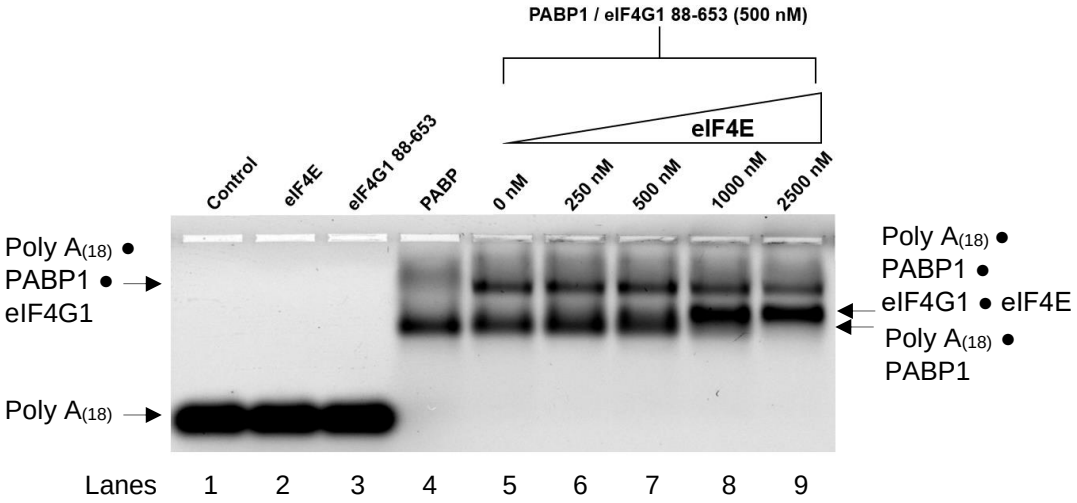

Figure 3.3: Gel shift assays of Poly $A_{(18)}$ ± PABP1, eIF4G1, & eIF4E. 0.7 % agarose gel. Binding of 100 nM Poly $A_{(18)}$ to 500 nM PABP1 and 500 nM eIF4G1 88-653 with an increasing concentration of eIF4E. RNA was 3' labeled with fluorescein.

3.3 m^7G – eIF4E – eIF4G1 – PABP1 complex

Next, we looked to see if it was possible to form the PABP1 ● eIF4G1 ● eIF4E complex in the absence of a Poly A tail but presence of the m^7G cap. For this experiment, we performed a gel shift assay with a short 17 nucleotide capped mRNA. The idea was to have only eIF4E bind to the capped mRNA while having the other components bind through RNA-independent interactions. As expected, our results showed a complete shift of the capped S17 mRNA by eIF4E, but not eIF4G1 88-653 (Figure 3.4, lanes 2-3). However, at the concentration used for this experiment, PABP1 exhibited some non-specific binding to the S17 mRNA (Figure 3.4, lane 4). Addition of eIF4G1 88-653 to the

S17 ● eIF4E complex induced a super-shift of the band which is indicative of the formation a S17 ● eIF4E ● eIF4G1 88-653 complex (Figure 3.4, lane 5).

Two additional observations can be made from this experiment. First, addition of PABP1 to the S17 ● eIF4E complex seemed to disrupt binding (Figure 3.4, lane 6). The fact that the specific interaction of eIF4E for the m^7G was disrupted by a non-specific interaction suggest that additional factors influence the stability of the m^7G ● eIF4E complex. Second, adding eIF4G1 88-653 to the S17, eIF4E, PABP1 sample rescued the S17 ● eIF4E interaction and induced a slight shift (Figure 3.4, lane 7). This new slightly shifted band could indicate the formation of a S17 ● eIF4E ● eIF4G1 88-653 ● PABP1 complex.

It is possible that eIF4G1 88-653 can enhance m^7G ● eIF4E complex formation through its association with eIF4E. Additionally, eIF4G1 88-653‘s interaction with PABP1 might alleviate the competitive interaction and promote a cooperation between all three proteins. Further studies would be required to determine if the m^7G ● eIF4E complex is influenced by eIF4G1 and PABP in an RNA-independent manner.

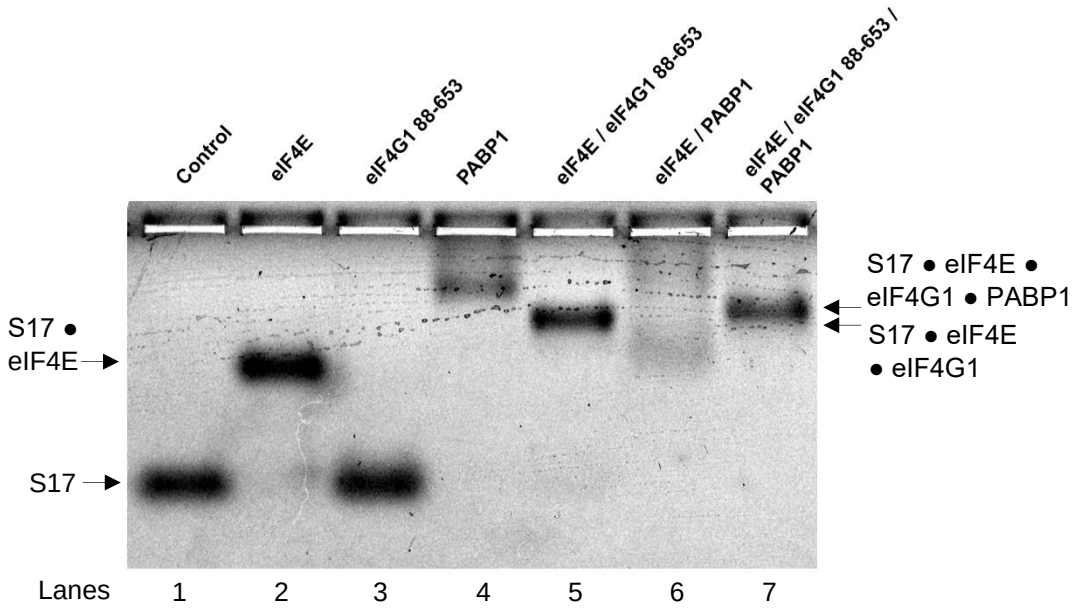

Figure 3.4: Gel shift assay of capped S17 mRNA. 0.7 % agarose gel. Binding of 10 nM capped S17 RNA to 1 µM eIF4E, 5 µM eIF4G1 88-653, and 5 µM PABP1. mRNA was 3' labeled with fluorescein.

3.4 mRNA – eIF4E – eIF4G1 complex affinity

We then wanted to determine if our eIF4G1 88-653 variant was able to enhance the affinity of the m^7G ● eIF4E complex. A previous study showed that an eIF4G1 variant lacking the central RNA binding domain (RBD) failed to enhance cross linking of eIF4E to the m^7G cap[33]. Additionally, a different study showed no significant difference in functional eIF4E binding to a cap analog in the presence of eIF4G1 557-646[28]. However, that same study reported that eIF4G1 does enhance binding of initially non-functional eIF4E to the m^7G cap. They claimed that recombinant eIF4E that is purified incorrectly can contain a

large amount of misfolded and inactive protein. That misfolded and inactive protein can then be rescued and activated by eIF4G1. Based on these studies, we expected our eIF4G1 88-653 variant (which does not possess the central RBD) to have no effect on the affinity of the m^7G ● eIF4E complex.

We first tested whether our recombinant eIF4E was functional. We quantified the equilibrium dissociation constant (K_D) of eIF4E binding to fluorescein labeled capped S17 mRNA using fluorescence anisotropy (Figure 3.5 A). We found the equilibrium dissociation constant (K_D = 137.1 ± 17.4 nM) to be within the range of previously published values for functional eIF4E[24-26]. We then proceeded to test the binding of eIF4E to capped S17 mRNA in the presence of excess eIF4G1 88-653. Interestingly, we found a slight enhancement (K_D = 95.2 ± 10.8 nM) in the binding affinity of eIF4E for capped S17 mRNA (Figure 3.5 B). The sample with just eIF4G1 88-653 and S17 mRNA showed no change in anisotropy. Additionally, we previously showed no interaction between eIF4G1 88-653 and S17 mRNA in our gel shift assay (Figure 3.4, lane 3). Furthermore, the greater change in anisotropy suggest a larger complex interacting with capped S17 mRNA. This can be once again confirmed with our gel shift assay (Figure 3.4, lane 5). Therefore, we can be confident that this enhancement is a result of eIF4G1 88-653 interacting with eIF4E.

Our results suggest that aside from the significant enhancement provided by the central RBD, eIF4G1 is also able to enhance eIF4E's cap binding through additional mechanisms. This is important because it can help increase the

stability of the complex by providing additional anchoring points between components.

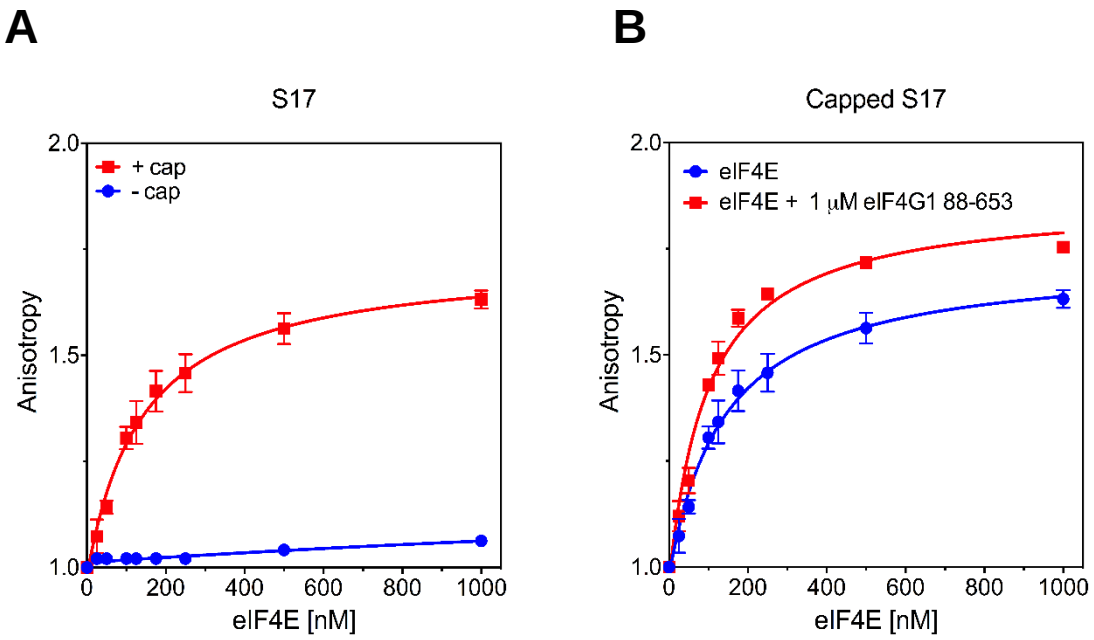

Figure 3.5: Fluorescence anisotropy measurements of eIF4E binding to S17 mRNA. (A) eIF4E titrated against 5 nM fluorescein-labeled S17 mRNA +/- m^7G cap. (B) eIF4E titrated against 5 nM capped fluorescein-labeled S17 mRNA in the presence and absence of 1 μM eIF4G1 88-653. All eIF4E binding trials were performed three times. Error bars depict standard deviation between trials.

Next, we looked at how the length of the mRNA might affect the m^7G ● eIF4E ● eIF4G1 complex formation. We used two different model mRNAs for our studies: M35 (a 35-nucleotide mRNA with a 5' m^7G cap) and CRC1 (a 114-nucleotide mRNA with a 5' m^7G cap and 3' 25 nucleotide Poly A tail). Gel shift assays were performed with each mRNA by titrating an increasing concentration of eIF4E in the presence and absence of two different central RBD deficient eIF4G1 variants (Figure 3.6 A & B). For both mRNAs, eIF4E was able to induce a complete shift at higher concentrations. Additionally, in the presence of the central RBD deficient eIF4G1 variants, a super-shift can be observed. This super-shift corresponds to the mRNA ● eIF4E ● eIF4G1 complex. Results for both mRNAs were nearly identical, which might suggest that the mRNA ● eIF4E ● eIF4G1 complex may form independent of mRNA length. However, the possibility does exist that longer mRNAs might behave differently and may require the central RBD missing from our variants.

Another interesting observation can be made regarding the formation of the mRNA ● eIF4E ● eIF4G1 complex (Figure 3.6 A & B). At excess eIF4G1 concentrations, the mRNA ● eIF4E ● eIF4G1 complex is the dominant species for both eIF4G1 variants. However, at equimolar concentrations of eIF4E and eIF4G1, the mRNA ● eIF4E complex is favored in the sample containing the shorter (MBP-eIF4G1 565-653) but not the longer (eIF4G1 88-653) variant. This is observed in both CRC1 and M35 mRNAs.

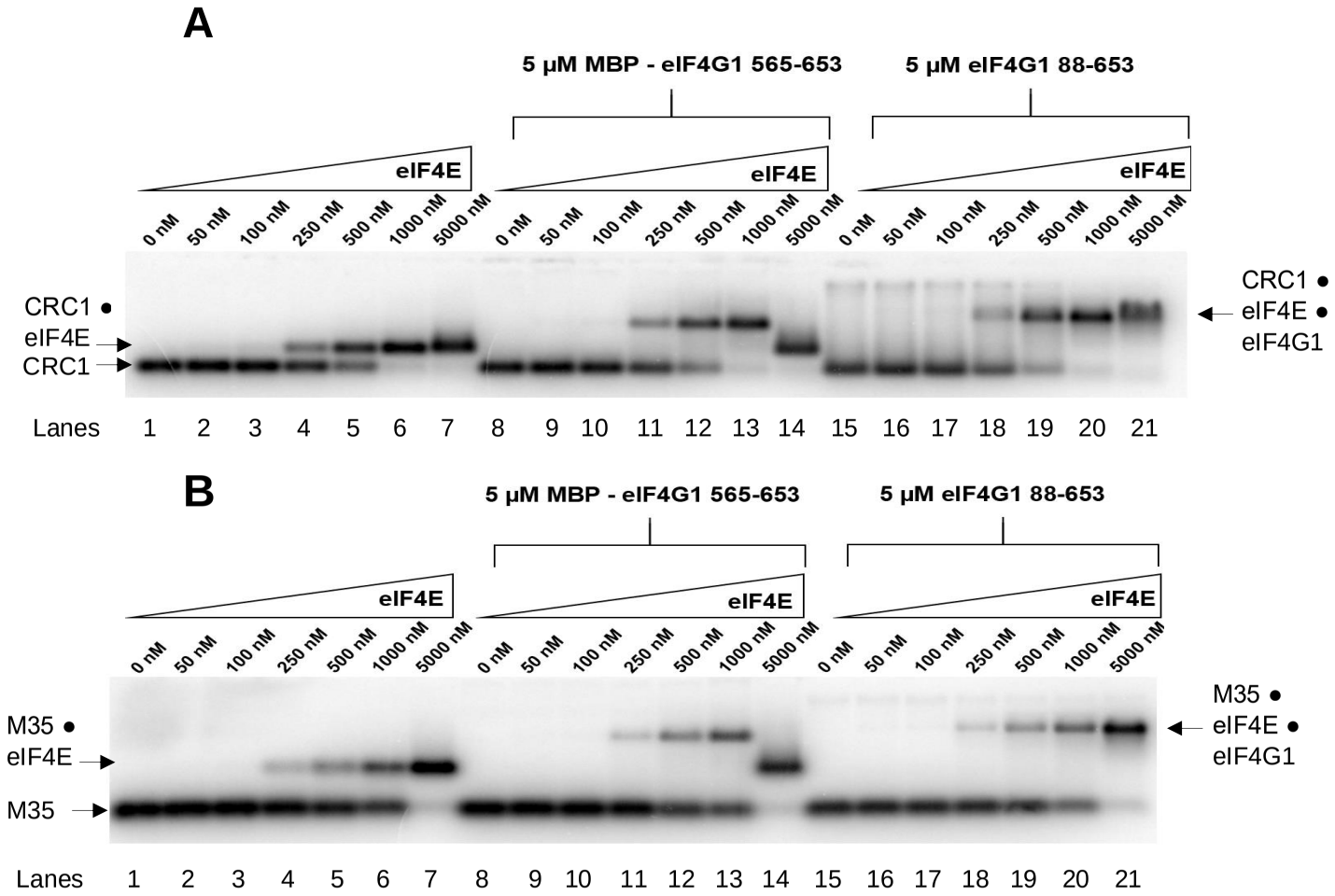

Figure 3.6: Gel shift assays of capped CRC1 and M35 +/- eIF4E and eIF4G1 variants. 1.5 % agarose gel (A) Binding of 100 nM capped CRC1 mRNA to eIF4E in the presence and absence of eIF4G1 variants (B) Binding of 500 nM capped M35 mRNA to eIF4E in the presence and absence of eIF4G1 variants. mRNA was internally labeled with α^{32}P UTP or ATP.

We then asked the question: is there an essential feature in the longer variant (eIF4G1 88-653) that allows for the preferential selection of mRNA bound eIF4E? We tested this using a gel shift assay with capped CRC1 mRNA (Figure 3.7). In this experiment, eIF4E was kept at a constant saturating concentration and three different eIF4G1 variants were titrated. As the concentration of eIF4G1 variants increased, the complex shifted from mRNA ● eIF4E to mRNA ● eIF4E ● eIF4G1. For MBP-eIF4G1 565-653, we observed the mRNA ● eIF4E ● eIF4G1 complex form at higher concentrations. However, the longer variants (eIF4G1 190-653, 88-653) promoted mRNA ● eIF4E ● eIF4G1 complex formation at lower concentrations. These results suggest that the N-terminal region may play a role in enhancing eIF4G1's affinity for mRNA bound eIF4E. This may provide an additional way of ensuring the stability of the messenger ribonucleoprotein complex.

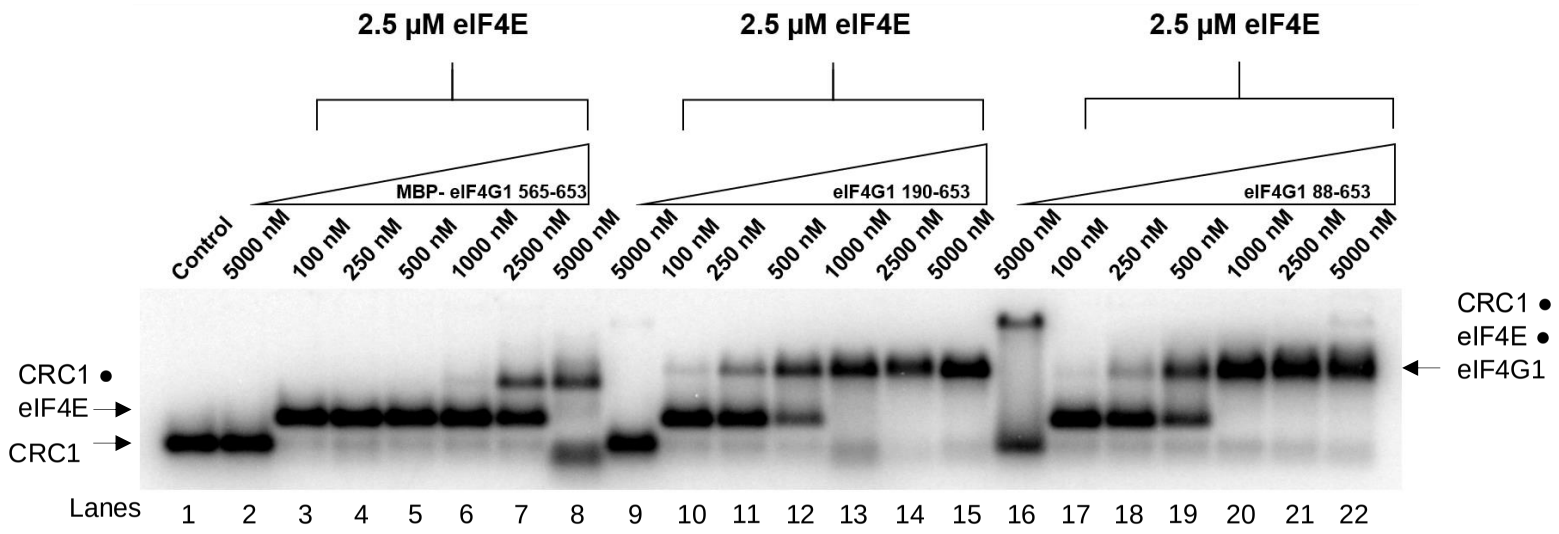

Figure 3.7: Gel shift assay of capped CRC1 with excess eIF4E and titration of eIF4G1 variants. 1.5 % agarose gel. Binding of 250 nM capped CRC1 mRNA with saturating eIF4E and increasing concentration of eIF4G1 variants. mRNA was internally labeled with α^{32}P UTP or ATP.

3.5 mRNA – eIF4E – eIF4G1 – PABP complex

Next, we looked at the formation of the mRNA (m^7G capped and Poly $A_{(25)}$ tailed) ● eIF4E ● eIF4G1 ● PABP1 complex using gel shift assays. An uncapped CRC1 mRNA was used as a control to show that eIF4E would not interact with an mRNA lacking the 5' m^7G cap (Figure 3.8, lane 2). Thus, preventing the formation of the "closed-loop" messenger ribonucleoprotein complex (Figure 3.8, lanes 3-5). For capped CRC1, eIF4E and PABP1 were kept at constant equimolar concentrations. Titration of eIF4G1 88-653 lead to the appearance of a new shifted band (Figure 3.8, lanes 6-14). Given the absence of this band in the sample lacking the 5' m^7G cap, it is likely indicative of an mRNA bound by eIF4E at the 5' cap, PABP1 at the 3' Poly A tail, and eIF4G1.

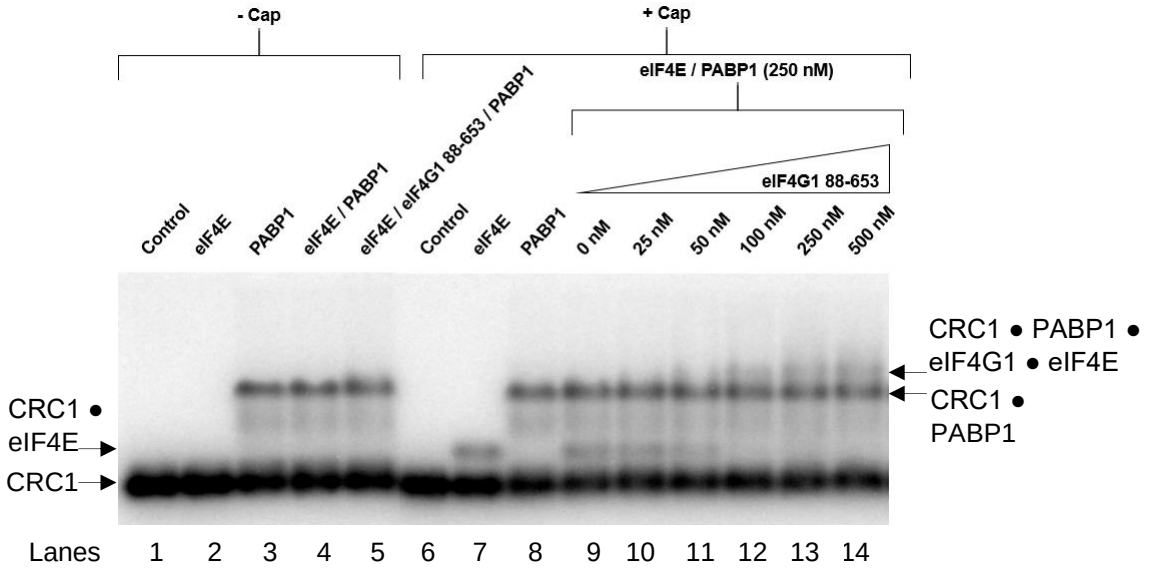

Figure 3.8: Gel shift assay of CRC1 +/- cap with initiation factors. 0.7 % agarose gel. Binding of 250 nM uncapped CRC1 mRNA to 250 nM eIF4E, eIF4G1 88-653, and PABP1. For capped CRC1 mRNA, eIF4G1 88-653 was titrated while keeping the eIF4E and PABP1 concentrations constant. mRNA was internally labeled with $\alpha^{32}P$ UTP or ATP.

We then verified that the new band was a complex consisting of all three proteins (eIF4E, eIF4G1, PABP1) and not an mRNA ● eIF4E ● eIF4G1 complex. Figure 3.9 shows the migration of different complexes relative to each other. These results show the mRNA ● eIF4E ● eIF4G1 complex migrating further down the gel relative to the mRNA ● PABP and mRNA ● eIF4E ● eIF4G1 complex. This suggest that the new shifted band (Figure 3.8, lanes 10-14) is a complex consisting of all three proteins (eIF4E, eIF4G1, PABP1).

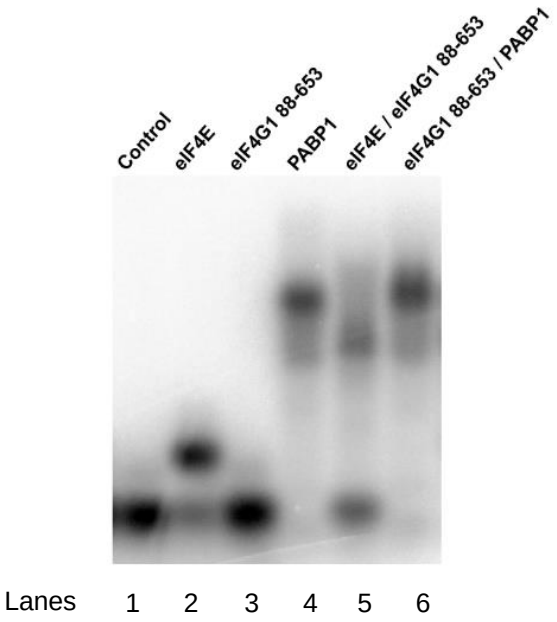

Figure 3.9: Gel shift assay of capped CRC1 with initiation factors. 1.5 % agarose gel. Binding of 125 nM capped CRC1 mRNA to 500 nM eIF4E, eIF4G1 88-653, and PABP1. mRNA was internally labeled with α^{32}P UTP or ATP.

Next, we further confirmed that the new band was an mRNA bound by eIF4E, eIF4G1, and PABP1. We performed a gel shift assay using different eIF4G1 variants. As previously mentioned, the MBP fusion was intentionally left on two of these shorter variants (eIF4G1 69-214, 565-653) to mimic the size and isoelectric point of the larger variants (eIFG1 190-653, 88-653). This would ensure a similar migration and allow for a better comparison between the samples.

Figure 3.10 shows the complexes formed by PABP1, eIF4E, and eIF4G1 variants with CRC1 mRNA (± m^7G cap). As expected, several differences can be observed between the eIF4G1 variants. Similarly, differences between complexes formed in the presence and absence of the 5' m^7G cap are evident. For all samples lacking the 5' m^7G cap, there is one predominant band regardless of the eIF4G1 variant used. Though two of the variants (eIF4G1 69-214, 88-653) bind PABP1, the resolution in this gel is not enough to distinguish an mRNA ● PABP1 complex from an mRNA ● PABP1 ● eIF4G1 complex. Additionally, eIF4E is unable to directly interact with the uncapped mRNA and only one of the variants (eIF4G1 88-653) can bind to both eIF4E and PABP1. Any eIF4E in complex would be a result of an eIF4G1 88-653 mediated interaction (Figure 3.11 A). However, the absence of another band suggest that this complex is likely not forming.

The appearance of a second band is evident in samples containing a 5' m^7G capped mRNA (Figure 3.10, lanes 5-10). Interestingly, the new band is only

found in samples containing an eIF4G1 variant capable of binding to eIF4E. Additionally, the intensity of the band is dependent on the length of the eIF4G1 variant. This is consistent with previous results (Figure 3.7). However, the fact that the second band appears in samples containing an eIF4G1 variant incapable of binding to PABP1 presents a confounding result. A new question arises: is the "closed-loop" ribonucleoprotein complex truly forming or does this new complex represent an eIF4E ● eIF4G1 complex at the 5' end with a PABP1 bound to the 3' end (Figure 3.11 B & C).

Further assays and a structure would be needed to definitively demonstrate the formation of a "closed-loop" ribonucleoprotein complex. However, the possibility does exist that additional components (apart from the eIF4E and PABP1 binding sites on eIF4G1) may be required for the formation of the "closed-loop" complex.

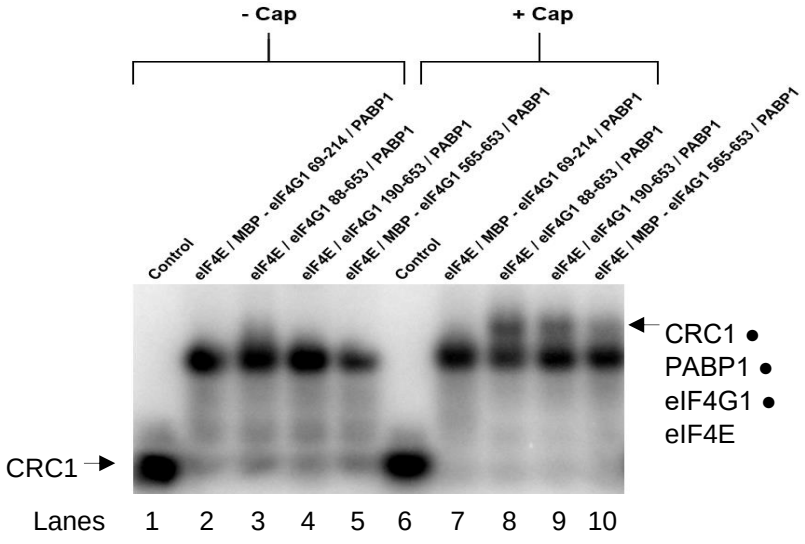

Figure 3.10: Gel shift assay of CRC1 +/- cap with initiation factors and different eIF4G1 variants. 1.5 % agarose gel. Binding of 250 nM CRC1 mRNA to 1 µM eIF4E, 1 µM eIF4G1 variants, and 1 µM PABP1. mRNA was internally labeled with α^{32}P UTP.

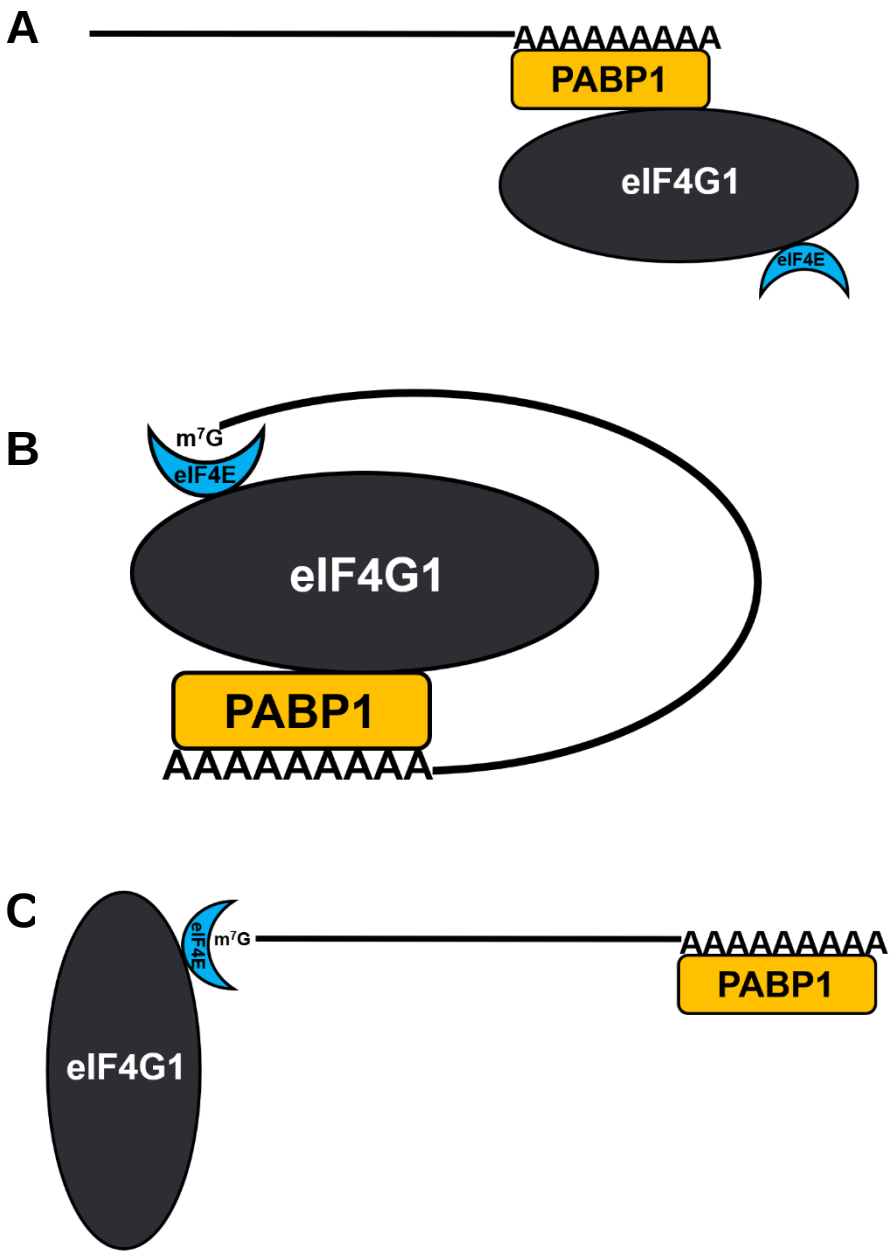

Figure 3.11: Possible ribonucleoprotein complexes (A) Uncapped mRNA bound by PABP1, eIF4G1, and eIF4E (B) mRNA bound by eIF4E, eIF4G1, and PABP1 through a “closed-loop” complex (C) mRNA bound by eIF4E, eIF4G1, and PABP1 without the formation of a “closed-loop” complex.

3.6 eIF4G1 RNA binding

Previous studies have shown human eIF4G1 to possess two RNA-binding domains in its central region (Figure 2.1 A)[33,34]. Furthermore, one of those studies showed no RNA binding by the N-terminal region of eIF4G1 using a gel shift assay of an eIF4G1 197-674 variant with β-globin RNA[33]. Here, we present evidence that suggests human eIF4G1 may possess an N-terminal RNA-binding domain.

We first tested RNA binding of four N-terminal eIF4G1 variants using a gel shift assay with 1000-nucleotide Renilla luciferase mRNA (Figure 3.12 A). Interestingly, we observed a shift with the eIF4G1 88-653 variant but not with any of the other variants. This suggests that RNA-binding could be influenced by multiple, as opposed to one region within the variant. It may be possible that eIF4G1 folds in a specific way which allows distant regions (relative to amino acid number) to be in proximity to allow for RNA binding.

Next, we tested RNA binding of the four N-terminal eIF4G1 variants with a shorter 114-nucleotide CRC1 mRNA (Figure 3.12 B). Surprisingly, using the same concentrations of mRNA and protein as before, there was no shift with any of the variants. However, at higher concentrations, we can observe a shift for eIF4G1 88-653 (Figure 3.7, lane 16). This suggest that the affinity of eIF4G1 88-653 for Renilla luciferase mRNA is significantly higher than for CRC1.

These results generate new questions regarding the RNA-binding activity of the N-terminal region of eIF4G1. First, why is the affinity for the two mRNAs tested significantly different and how is eIF4G1 discriminating between the two? It may be possible that this RNA-binding activity is dependent on the length of the RNA. Alternatively, it may recognize a specific sequence or secondary structure within the RNA. Furthermore, what is the biological significance of this N-terminal RNA binding domain? If indeed it is a length dependent interaction, it may act as an additional anchoring point to ensure the stability of the messenger ribonucleoprotein complex with larger mRNAs. Further experiments and a structure would be needed to gain insight on the purpose and mechanism of RNA binding by the N-terminal region of eIF4G1.

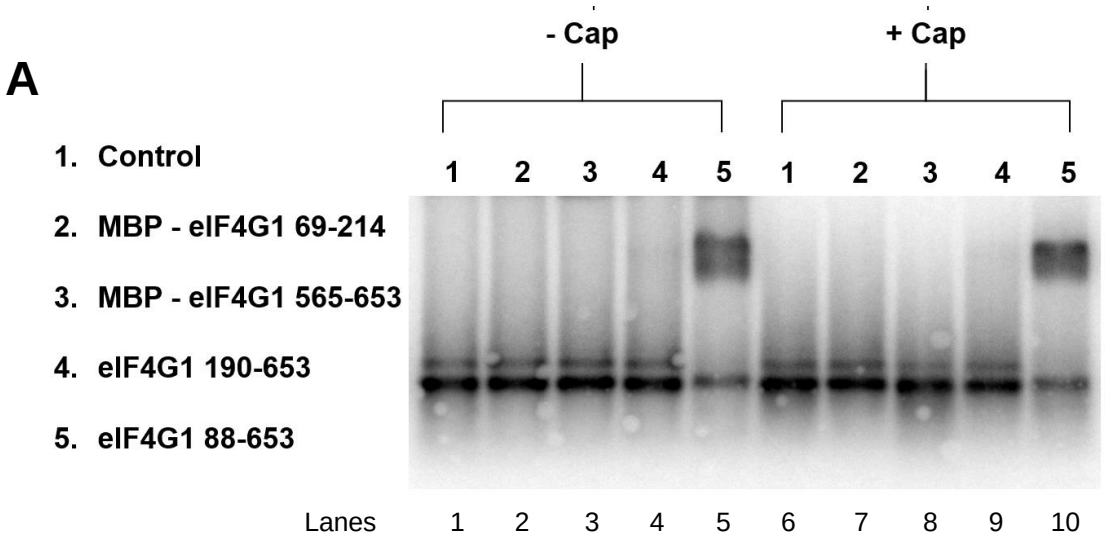

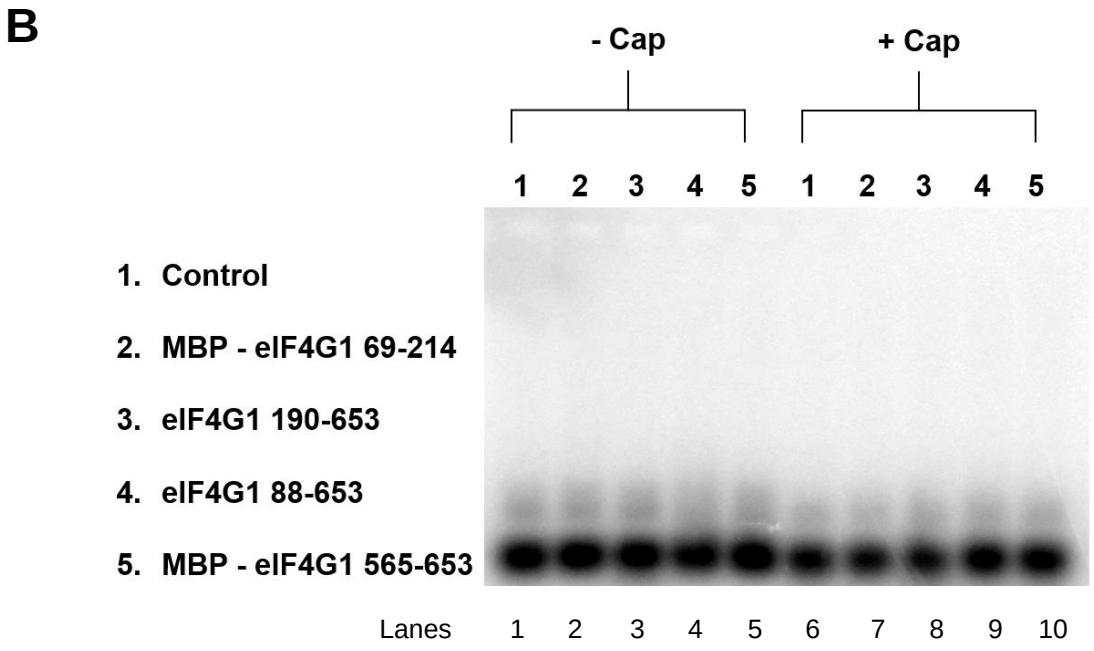

Figure 3.12: Gel shift assays of Renilla luciferase and CRC1 mRNA with eIF4G1 variants. 1.5 % agarose gel (A) Binding of 50 nM Renilla luciferase mRNA with 500 nM eIF4G1 variants. (B) Binding of 50 nM CRC1 mRNA with 500 nM eIF4G1 variants. mRNA was internally labeled with α^{32}P UTP or ATP.

Chapter 4: Conclusions and Future Directions

4.1 Test binding affinity of eIF4E to the m^7G cap in the presence of eIF4G1 variants and PABP1 using fluorescence anisotropy

It was interesting to see an enhancement in the affinity of eIF4E for the m^7G cap in the presence of an eIF4G1 variant lacking the middle RNA binding domain. However, it is unclear whether this is a result of eIF4G1 binding to eIF4E through its known binding domains or if the N-terminal region also plays a role. We plan to test this using an N-terminal truncated eIF4G1 variant. Additionally, we would like to see the influence that PABP1●eIF4G1 complex has on the affinity of eIF4E for the m^7G cap. Finally, we would like to see how that interaction differs for a poly A bound PABP1.

4.2 Isolate and solve the structure of the eIF4E●eIF4G1●PABP1●mRNA Complex

While the “closed-loop” ribonucleoprotein structure has been demonstrated in yeast, additional evidence is needed for the human complex. Though our gel shift assays showed the formation of a complex consisting of all components, we could not conclude if the complex was indeed a “closed-loop” structure. We plan to isolate the eIF4E●eIF4G1●PABP1●mRNA complex and

solve the structure using cryo-EM. This will provide evidence for the formation of the “closed-loop” structure in humans.

4.3 Express and purify full length human eIF4G1

Though variants are a great way of demonstrating interactions between different components, they cannot account for the potential difference in behavior for a full-length protein. For that reason, we plan to express and purify full-length human eIF4G1. We hope that using the full-length protein will provide greater insights into the human translation initiation complex.

Chapter 5: Materials and Methods

5.1 Expression and purification of human eIF4G1 variants

The human eIF4G1 isoform 5 (NP_937884.1) gene (coding from amino acid 88-653) was codon optimized for *E. coli* expression and purchased as a FragmentGENE (GENEWIZ). The gene coding for eIF4G1 88-653 was subcloned using NdeI and SapI sites into the pTXB1 vector (NEB) which contains a C-terminal Mxe GyrA Intein and a chitin binding domain. An additional threonine was inserted after D653 to enhance cleavage during purification. The eIF4G1 190-653 variant was generated from the eIF4G1 88-653 (pTXB1) plasmid via PCR deletion mutagenesis. The eIF4G1 88-214 and eIF4G1 565-653 variant were subcloned into the LIC expression vector pMCSG9 (DNASU plasmid repository) which contains a N-terminal hexahistidine-MBP fusion tag that is cleavable by TEV protease. To generate eIF4G1 69-214, a codon optimized gene sequence coding for amino acids 69-87 was inserted into the eIF4G1 88-214 (pMCSG9) plasmid via PCR insertion mutagenesis.

The eIF4G1 88-653, eIF4G1 190-653, MBP-eIF4G1 69-214, and MBP-eIF4G1 565-653 expression plasmids were transformed into *E. coli* BL21 (DE3) Star cells (Novagen). Cells were grown overnight at 37°C in a 5 ml LB starter culture supplemented with 100 µg/mL ampicillin. A 1 L LB media containing 100 µg/mL ampicillin was inoculated with 3-5 ml of the overnight starter culture and

grown at 37°C to OD_{600} ~0.5. The culture was cooled to 30°C then induced with 0.4 mM IPTG and grown at that temperature for 2.5 – 3 hrs. Cells were pelleted at 5000 RPM for 15 min at 4°C and then stored at -80°C.

Cells expressing eIF4G1 88-653 and eIF4G1 190-653 were resuspended in pTXB1 lysis buffer (20 mM Hepes, 100 mM NaCl, 10% Glycerol, 1 mM PMSF, pH 8.5) at approximately 20 ml per gram of pellet, then lysed by French Press. Lysate was clarified at 50,000g for 30 min at 4°C then load onto a pre-equilibrated column containing chitin resin (NEB) with a flow rate of ~0.5 ml/min at 4°C. The resin was washed with 10 column volumes of pTXB1 lysis buffer, 10 column volumes of pTXB1 wash buffer (20 mM Hepes, 1M NaCl, 10% Glycerol, 1 mg/ml Heparin sodium salt, pH 8.5), then an additional 10 column volumes of pTXB1 lysis buffer. The resin was then quickly washed with 3 column volumes of cleavage buffer (20 mM Hepes, 100 mM NaCl, 10% Glycerol, 50 mM DTT, pH 8.5) before closing and allowed to incubate in cleavage buffer for 16-20 hrs at room temperature. Fractions were collected, analyzed by SDS-PAGE, then pooled and concentrated to ~5 ml in an Amicon Ultra Centrifugal Filter (Millipore). Proteins were further purified on a Superdex 75 16/60 gel filtration column (GE Healthcare) in Buffer A (20 mM Tris-HCl, 100 mM KCl, 5% Glycerol, 2 mM DTT, pH 7.5). Fractions were analyzed by SDS-PAGE and only the purest fractions were pooled, concentrated, aliquoted, flash-frozen, and stored at -80°C.

Cells expressing MBP-eIF4G1 69-214 and MBP-eIF4G1 565-653 were resuspended in Ni-NTA lysis buffer (100 mM Tris-HCl, 100 mM KCl, 5% Glycerol,

5 mM Imidazole, 5 mM β-mercaptoethanol, 1 mM PMSF, pH 8.0) then lysed by sonication (12 cycles of 8 second pulse with 1 min rest). Lysate was clarified at 50,000g for 30 min at 4°C then loaded onto a pre-equilibrated column containing Ni-NTA resin (MCLAB) with a flow rate of ~0.5 ml/min. The resin was washed with 50 column volumes of Ni-NTA stringent wash buffer (100 mM Tris-HCl, 1 M KCl, 5% Glycerol, 20 mM Imidazole, 5 mM β-mercaptoethanol, 1 mg/ml Heparin sodium salt pH 8.0) followed by 50 column volumes of Ni-NTA wash buffer (100 mM Tris-HCl, 100 mM KCl, 5% Glycerol, 20 mM Imidazole, 5 mM β-mercaptoethanol, pH 8.0). Protein was eluted in Ni-NTA elution buffer (20 mM Tris-HCl, 100 mM KCl, 5% Glycerol, 250 mM Imidazole, pH 8.0) and fractions analyzed by SDS-PAGE. Fractions containing protein were pooled together, concentrated to ~5 ml, and dialyzed overnight at 4°C into Buffer A using Spectra/Por 6-8 kD MWCO dialysis tubing (Spectrum). Protein was then concentrated, aliquoted, flash-frozen, and stored at -80°C.

5.2 Expression and purification of human eIF4E

A plasmid with the gene coding for human eIF4E isoform 1 (NP_001959.1) was purchased (Addgene plasmid 17343) and subcloned into the LIC expression vector pMCSG26 (DNASU plasmid repository) which contains a C-terminal hexahistidine fusion tag[57]. The eIF4E (pMCSG26) plasmid was then transformed into *E. coli* Rosetta 2 (DE2) pLysS cells (Novagen). Cells were

grown overnight at 37°C in a 5 ml LB starter culture supplemented with 100 µg/mL ampicillin and 25 µg/mL chloramphenicol . A 1 L LB media containing 100 µg/mL ampicillin and 25 µg/mL chloramphenicol was inoculated with 3-5 ml of the overnight starter culture and grown at 37°C to OD_{600} ~0.5. The culture was cooled to 16°C then induced with 0.2 mM IPTG and grown at that temperature for ~16 hrs. Cells were pelleted at 5000 RPM for 15 min at 4°C and then stored at -80°C.

Cells expressing eIF4E were resuspended in Ni-NTA lysis buffer (100 mM Tris-HCl, 100 mM KCl, 5% Glycerol, 5 mM Imidazole, 5 mM β-mercaptoethanol, 1 mM PMSF, pH 8.0) then lysed by French Press. Lysate was clarified at 50,000g for 30 min at 4°C then loaded onto a pre-equilibrated column containing Ni-NTA resin (MCLAB) with a flow rate of ~0.5 ml/min. The resin was washed with 50 column volumes of Ni-NTA stringent wash buffer (100 mM Tris-HCl, 1 M KCl, 5% Glycerol, 20 mM Imidazole, 5 mM β-mercaptoethanol, 1 mg/ml Heparin sodium salt pH 8.0) followed by 50 column volumes of Ni-NTA wash buffer (100 mM Tris-HCl, 100 mM KCl, 5% Glycerol, 20 mM Imidazole, 5 mM β-mercaptoethanol, pH 8.0). Protein was eluted in Ni-NTA elution buffer (20 mM Tris-HCl, 100 mM KCl, 5% Glycerol, 250 mM Imidazole, pH 8.0) and fractions analyzed by SDS-PAGE. Fractions containing protein were pooled together, concentrated to ~5 ml, and further purified on a Superdex 75 16/60 gel filtration column (GE Healthcare) in Buffer A (20 mM Tris-HCl, 100 mM KCl, 5% Glycerol, 2 mM DTT, pH 7.5). Fractions were analyzed by SDS-PAGE and only the

fractions corresponding to monomeric protein were pooled, concentrated, aliquoted, flash-frozen, and stored at -80°C.

5.3 In vitro transcription of RNA

Full length Renilla luciferase mRNA was produced by in vitro transcription (IVT) using T7 RNA polymerase. The sequence coding for full length Renilla luciferase mRNA was PCR amplified to generate a linear template with a 3' 25-nucleotide poly A tail for IVT. A 100 µl reaction was set up with a final concentration of 40 mM Tris pH 8.0, 20 mM $MgCl_2$, 2 mM spermidine, 0.1% Triton X-100, 5 mM DTT, 4 mM of each NTP, 8 µg of linear PCR template, T7 RNA polymerase, and 2 µl of 10 µCi/µl [α-^{32}P] ATP or UTP (for radioactively labeled mRNA only). The reaction was incubated at 37°C for 6 hours and then purified using an RNA clean-up and concentration kit (Norgen Biotek or Monarch NEB). The RNA concentration was measured by its 260 nm absorbance in a NanoDrop 2000 Spectrophotometer and then stored at -80°C.

The sequence coding for CRC1 mRNA was produced by removing a large middle portion of full length Renilla luciferase through PCR deletion mutagenesis. The sequence coding for CRC1 mRNA was then PCR amplified to generate a linear template with a 3' 25-nucleotide poly A tail for IVT. CRC1 mRNA was produced by IVT using T7 RNA polymerase and under the same conditions as full length Renilla luciferase. After IVT, 100 µl of 2X formamide loading dye (95%

formamide, 20 mM EDTA, 0.05% xylene cyanol and 0.05% bromophenol blue) was added to the reaction, heated at 95°C for 2 min then loaded into a pre-run 1.5 mm thick 6% denaturing polyacrylamide gel (dPAGE). The gel was run at room temperature in 1X TBE (100 mM Tris, 100 mM Boric acid, 2 mM EDTA) for 2 hours at 30 watts. The RNA was then visualized by UV shadowing. The RNA band was excised from the gel with a razor, cut into pieces, then placed in a 1.5 ml Eppendorf tube. The RNA was extracted by adding 600 µl of RNA elution buffer (0.5 M sodium acetate pH 5.2, 0.1 mM EDTA pH 8.0, 0.1% SDS) and placed in an Eppendorf 5432 mixer overnight at 4°C. The RNA was then purified by chloroform extraction (three 600 µl extractions) and ethanol precipitation at -80°C for a minimum of 1 hour. The sample was then centrifuged at 16000 x g for 30 minutes at 4 °C. The supernatant was then removed, and the RNA pellet was washed with 500 µl of 70% ethanol. The sample was then centrifuged at 16000 x g for 1 min. The supernatant was removed, and the RNA pellet was dried without heat for 5 minutes in a SpeedVac. The RNA pellet was then dissolved in 20 µl of RNase-free water. The RNA concentration was measured by its 260 nm absorbance in a NanoDrop 2000 Spectrophotometer and then stored at -80°C.

M35 and S17 RNAs were produced by IVT using DNA oligonucleotides as templates for transcription by T7 RNA polymerase. A top strand (18T7T) and bottom strand (coding strand) were annealed to generate a duplex template in the T7 promoter region which allows for the initiation of transcription by T7 RNA polymerase. For annealing, 1000 picomoles of 18T7T and 1000 picomoles of the

coding strand were mixed in a final volume of 20 µl, heated to 95°C for 2 min, and then slow cooled to room temperature. A 100 µl reaction was set up with a final volume of 100 mg/ml PEG800, 40 mM Tris pH 8.1, 2 mM spermine, 5 mM DTT, 0.01% Triton X-100, 4 mM of each NTP, 20 mM $MgCl_2$, 4 µl of annealed template, T7 RNA polymerase, and 2 µl of 10 µCi/µl [α-^{32}P] ATP or UTP (for radioactively labeled mRNA only). The reaction was incubated at 37°C for 6 hrs. After IVT, the RNA was purified on a 12% dPAGE as described for CRC1.

5.4 Labeling the RNA 3' end with fluorescein 5-thiosemicarbizide

S17 was labeled at the 3' end with fluorescein 5-thiosemicarbide (FTSC). First, the 3' end of the RNA was oxidized for 90 minutes at room temperature in a 50 µl reaction containing 100 mM sodium acetate (NaOAc) pH 5.2, 100 µM potassium periodate (KIO_4), and 0.5 nmoles of RNA. Oxidized RNA was precipitated by adding 2.5 µl of 5M NaCl, 2 µl of 10mg/ml glycogen, 100 µl of 100% ethanol, and incubating at -20°C for 20 min. The RNA was pelleted at 16000 x g at 4°C for 25 min. The supernatant was removed, and the pellet was air dried for 5 min before being resuspended in 50 µl of FTSC labeling solution (100 mM NaOAc pH 5.2, 1.5 mM FTSC). The reaction was incubated at 4°C overnight in the dark. The RNA was then precipitated by adding 5 µl of 3 M NaOAc pH 5.2, 140 µl of 100% ethanol, and incubating at least 30 min at -20°C. The RNA was pelleted at 16000 x g at 4°C for 25 min. The supernatant was

removed, and the pellet was washed with 150 µl of 70% ethanol. The RNA was pelleted once more then resuspended in 20 µl of RNase-free water.

5.5 Capping Reaction

For capping, RNA was first heated at 65°C for 5 min then placed on ice for an additional 5 min. The RNA was then incubated at 37°C for 2 hours in a reaction containing a final concentration of 50 mM Tris pH 8.0, 5 mM KCl, 1 mM $MgCl_2$, 1 mM DTT, 0.5 mM GTP, 0.1 mM S-adenosylmethionine (SAM), and vaccinia capping enzyme (ratio of enzyme to RNA varied from 1:10 to 1:100). The RNA was then purified using a Monarch nucleic acid purification kit (NEB). Capped RNA was stored in RNase-free water at -80°C.

5.6 Electrophoretic mobility shift assay (EMSAs or gel-shift assays)

Reactions were incubated in binding buffer (50 mM Tris pH 8.0, 70 mM KCl, 1 mM DTT, 0.01% Tween20, 50 ng/µl total tRNA from *E. coli*) and 1 µl of xylene cyanol loading dye (50% glycerol, 0.25% xylene cyanol) in a final volume of 10 µl for 1 hour at room temperature. Reactions were then loaded into a SeaKem GTG Agarose (Lonza) gel in 1X TBE. The gels were run at 66V for ~2 hours at 4°C in a tray surrounded by ice. Fluorescein labeled RNA gels were then visualized using a Typhoon FLA9500. Radioactively labeled RNA gels were

incubated in gel fixing solution (20% Methanol, 10% Glacial Acetic Acid) for 15 min before vacuum drying for 60 min at 80°C on a Hybond N+membrane (Amersham, Fisher Scientific) and a sheet of Whatman paper. Dried gels were exposed to a phosphorimager screen overnight then visualized using a Typhoon FLA9500.

5.7 Fluorescence anisotropy binding assay

Reactions were incubated in binding buffer (50 mM Tris pH 8.0, 150 mM KCl, 1 mM DTT, 0.01% Tween20, 50 ng/µl total tRNA from *E. coli*) in a final volume of 100 µl for 1 hour at room temperature. Samples were measured in a non-binding 96 well plate using a Tecan Safire 2 plate reader by exciting at 470 nm and emission measured at 520 nm with a 10 nm bandwidth. Anisotropy data was analyzed using GraphPad Prism.

References

1. Jaiswal, P. K., Koul, S., Shanmugam, P. S. T., & Koul, H. K. (2018). Eukaryotic Translation Initiation Factor 4 Gamma 1 (eIF4G1) is upregulated during Prostate cancer progression and modulates cell growth and metastasis. Scientific Reports, (March), 1–12.

2. Howard, A., & Rogers, A. N. (2014). Role of translation initiation factor 4G in lifespan regulation and age-related health. Ageing Research Reviews, 13(1), 115–124.

3. De Benedetti, A., & Graff, J. R. (2004). eIF-4E expression and its role in malignancies and metastases. Oncogene, 23(18), 3189–3199.

4. Wendel, H. G., Silva, R. L. A., Malina, A., Mills, J. R., Zhu, H., Ueda, T., Watanabe-Fukunaga, R., Fukunaga, R., Teruya-Feldstein, J., Pelletier, J., & Lowe, S. W. (2007). Dissecting eIF4E action in tumorigenesis. Genes and Development, 21(24), 3232–3237.

5. Panthu, B., Terrier, O., Carron, C., Traversier, A., Corbin, A., Balvay, L., Lina, B., Rosa-Calatrava, M., & Ohlmann, T. (2017). The NS1 Protein from Influenza Virus Stimulates Translation Initiation by Enhancing Ribosome Recruitment to mRNAs. *Journal of Molecular Biology*, 429(21), 3334–3352.

6. Feigenblum, D., & Schneider, R. J. (1993). Modification of eukaryotic initiation factor 4F during infection by influenza virus. Journal of Virology, 67(6), 3027–3035.

7. Lomakin, I. B., Hellen, C. U., & Pestova, T. V. (2000). Physical association of eukaryotic initiation factor 4G (eIF4G) with eIF4A strongly enhances binding of eIF4G to the internal ribosomal entry site of encephalomyocarditis virus and is required for internal initiation of translation. *Molecular and Cellular Biology*, 20(16), 6019–6029.

8. Saleh, L., Rust, R. C., Fullkrug, R., Beck, E., Bassili, G., Ochs, K., & Niepmann, M. (2001). Functional interaction of translation initiation factor eIF4G with the foot-and-mouth disease virus internal ribosome entry site. *J Gen.Virol*., 82(Pt 4), 757–763.

9. Arias-Mireles, B. H., De Rozieres, C. M., Ly, K., & Joseph, S. (2018). RNA Modulates the Interaction between Influenza A Virus NS1 and Human PABP1. Biochemistry, 57(26), 3590–3598. research-article.

10. Lee, K. a, & Sonenberg, N. (1982). Inactivation of cap-binding proteins accompanies the shut-off of host protein synthesis by poliovirus. Proceedings of the National Academy of Sciences of the United States of America, 79(11),

11. Haghighat, A., Svitkin, Y., Novoa, I., Kuechler, E., Skern, T., & Sonenberg, N. (1996). The eIF4G-eIF4E Complex Is the Target for Direct Cleavage by the Rhinovirus 2A Proteinase. Journal of Virology, 70(12), 8444–8450.

12. Kentsis, A., Dwyer, E. C., Perez, J. M., Sharma, M., Chen, A., Pan, Z. Q., & Borden, K. L. B. (2001). The RING domains of the promyelocytic leukemia protein PML and the arenaviral protein Z repress translation by directly inhibiting translation initiation factor eIF4E. Journal of Molecular Biology, 312(4), 609–623.

13. Pelletier, J., Graff, J., Ruggero, D., & Sonenberg, N. (2015). Targeting the eIF4F translation initiation complex: A critical nexus for cancer development. *Cancer Research*, *75*(2), 250–263.

14. Karaki, S., Andrieu, C., Ziouziou, H., & Rocchi, P. (2015). The Eukaryotic Translation Initiation Factor 4E (eIF4E) as a Therapeutic Target for Cancer. Advances in Protein Chemistry and Structural Biology (1st ed., Vol. 101). Elsevier Inc.

15. Yuan, S., Chu, H., Ye, J., Hu, M., Singh, K., Chow, B. K. C., Zhou, J., & Zheng, B. J. (2016). Peptide-Mediated Interference of PB2-eIF4G1 Interaction Inhibits Influenza A Viruses' Replication in Vitro and in Vivo. ACS Infectious Diseases, 2(7), 471–477.

16. Lin, C. J., Nasr, Z., Premsrirut, P. K., Porco, J. A., Hippo, Y., Lowe, S. W., & Pelletier, J. (2012). Targeting Synthetic Lethal Interactions between Myc and the eIF4F Complex Impedes Tumorigenesis. Cell Reports, 1(4), 325–333.

17. Graff, J. R., Konicek, B. W., Carter, J. H., & Marcusson, E. G. (2008). Targeting the eukaryotic translation initiation factor 4E for cancer therapy. Cancer Research, 68(3), 631–634.

18. Sonenberg, N., & Hinnebusch, A. G. (2009). Regulation of Translation Initiation in Eukaryotes: Mechanisms and Biological Targets. *Cell*, 136(4), 731–745.

19. Marcotrigiano, J., Gingras, A. C., Sonenberg, N., & Burley, S. K. (1997). Cocrystal structure of the messenger RNA 5' cap-binding protein (eIF4E) bound to 7-methyl-GDP. *Cell*, 89(6), 951–961.

20. Lama, D., Pradhan, M. R., Brown, C. J., Eapen, R. S., Joseph, T. L., Kwoh, C. K., Lane, D. P. & Verma, C. S. (2017). Water-Bridge Mediates Recognition of mRNA Cap in eIF4E. *Structure*, 25(1), 188–194.

21. Siddiqui, N., Tempel, W., Nedyalkova, L., Volpon, L., Wernimont, A. K., Osborne, M. J., Hee-Won, P., & Borden, K. L. B. (2012). Structural insights into the allosteric effects of 4EBP1 on the eukaryotic translation initiation factor eIF4E. *Journal of Molecular Biology*, 415(5), 781–792.

22. Tomoo, K., Shen, X., Okabe, K., Nozoe, Y., Fukuhara, S., Morino, S., Ishida, T., Taniguchi, T., Hasegawa, H., Terashima, A., Sasaki, M., Katsuya, Y., Kitamura, K., Miyoshi, H., Ishikawa, M., & Miura, K. (2002). Crystal structures of 7-methylguanosine 5′-triphosphate (m7GTP)- and P1-7-methylguanosine-P3-adenosine-5′,5′-triphosphate (m7GpppA)-bound human full-length eukaryotic initiation factor 4E: biological importance of the C-terminal flexible region. *Biochemical Journal*, 362(3), 539–544.

23. Volpon, L., Osborne, M. J., Topisirovic, I., Siddiqui, N., & Borden, K. L. B. (2006). Cap-free structure of eIF4E suggests a basis for conformational regulation by its ligands. *EMBO Journal*, 25(21), 5138–5149.

24. Zuberek, J., Jemielity, J., Jablonowska, A., Stepinski, J., Dadlez, M., Stolarski, R., & Darzynkiewicz, E. (2004). Influence of Electric Charge Variation at Residues 209 and 159 on the Interaction of eIF4E with the mRNA 5′ Terminus. *Biochemistry*, 43(18), 5370–5379.

25. Friedland, D. E., Wooten, W. N. B., LaVoy, J. E., Hagedorn, C. H., & Goss, D. J. (2005). A mutant of eukaryotic protein synthesis initiation factor eIF4E K119A has an increased binding affinity for both m7G cap analogues and eIF4G peptides. *Biochemistry*, 44(11), 4546–4550.

26. Niedzwiecka, A., Marcotrigiano, J., Stepinski, J., Jankowska-Anyszka, M., Wyslouch-Cieszynska, A., Dadlez, M., Gingras, A., Pawel, M., Darzynkiewicz, E., Sonenberg, N., Burley, S. K., & Stolarski, R. (2002). Biophysical studies of eIF4E cap-binding protein: Recognition of mRNA 5′ cap structure and synthetic fragments of eIF4G and 4E-BP1 proteins. *Journal of Molecular Biology*, 319(3), 615–635.

27. Mader, S., Lee, H., Pause, A., & Sonenberg, N. (1995). The translation initiation factor eIF-4E binds to a common motif shared by the translation factor eIF-4 gamma and the translational repressors 4E-binding proteins. *Molecular and Cellular Biology*, 15(9), 4990–4997.

28. Slepenkov, S. V., Korneeva, N. L., & Rhoads, R. E. (2008). Kinetic Mechanism for Assembly of the m 7 GpppG·eIF4E·eIF4G Complex. *Journal of Biological Chemistry*, 283(37), 25227–25237.

29. Imataka, H., Gradi, A., & Sonenberg, N. (1998). A newly identified N-terminal amino acid sequence of human eIF4G binds poly(A)-binding protein and functions in poly(A)- dependent translation. *EMBO Journal*, 17(24), 7480–7489.

30. Safaee, N., Kozlov, G., Noronha, A. M., Xie, J., Wilds, C. J., & Gehring, K. (2012). Interdomain Allostery Promotes Assembly of the Poly(A) mRNA Complex with PABP and eIF4G. Molecular Cell, 48(3), 375–386.

31. Lamphear, B., Kirchweger, R., Skern, T., & Rhoads, R. (1995). Mapping of Functional Domains in Eukaryotic Protein Synthesis Initiation Factor 4G (eIF4G) with Picornaviral Proteases. Journal of Biological Chemistry, 270(37), 21975–21983.

32. Grüner, S., Peter, D., Weber, R., Wohlbold, L., Chung, M. Y., Weichenrieder, O., Valkov, E., Igreja, C., & Izaurralde, E. (2016). The Structures of eIF4E-eIF4G Complexes Reveal an Extended Interface to Regulate Translation Initiation. *Molecular Cell*, 64(3), 467–479.

33. Yanagiya, A., Svitkin, Y. V., Shibata, S., Mikami, S., Imataka, H., & Sonenberg, N. (2009). Requirement of RNA Binding of Mammalian Eukaryotic Translation Initiation Factor 4GI (eIF4GI) for Efficient Interaction of eIF4E with the mRNA Cap. *Molecular and Cellular Biology*, 29(6), 1661–1669.

34. Marcotrigiano, J., Lomakin, I. B., Sonenberg, N., Pestova, T. V., Hellen, C. U. T., & Burley, S. K. (2001). A conserved HEAT domain

within eIF4G Directs Assembly of the Translation Initiation Machinery. Molecular Cell, 7(1), 193–203.

35. Imataka, H., & Sonenberg, N. (1997). Human eukaryotic translation initiation factor 4G (eIF4G) possesses two separate and independent binding sites for eIF4A. Molecular and Cellular Biology, 17(12), 6940–6947.

36. Pestova, T. V, Shatsky, I. N., & Hellen, C. U. (1996). Functional dissection of eukaryotic initiation factor 4F: the 4A subunit and the central domain of the 4G subunit are sufficient to mediate internal entry of 43S preinitiation complexes. *Molecular and Cellular Biology*, 16(12), 6870–6878.

37. Marintchev, A., Edmonds, K. A., Marintcheva, B., Hendrickson, E., Oberer, M., Suzuki, C., Herdy, B., Sonenberg, N., & Wagner, G. (2009). Topology and Regulation of the Human eIF4A / 4G / 4H Helicase Complex in Translation Initiation. Cell, 136(3), 447–460.

38. Sawazaki, R., Imai, S., Yokogawa, M., Hosoda, N., Hoshino, S. I., Mio, M., Shimada, I., & Osawa, M. (2018). Characterization of the multimeric structure of poly(A)-binding protein on a poly(A) tail. Scientific Reports, 8(1), 1–13.

39. Hong, K. Y., Lee, S. H., Gu, S., Kim, E., An, S., Kwon, J., Lee, J., & Jang, S. K. (2017). The bent conformation of poly(A)-binding protein induced by RNA-binding is required for its translational activation function. RNA Biology, 14(3), 370–377.

40. Kahvejian, A., Svitkin, Y. V, Sukarieh, R., Boutchou, M. M., & Sonenberg, N. (2005). Mammalian poly (A) -binding protein is a eukaryotic translation initiation factor , which acts via multiple mechanisms. Genes and Development, 19, 104–113.

41. Baer, B. W., & Kornberg, R. D. (1983). The protein responsible for the repeating structure of cytoplasmic poly(A)-ribonucleoprotein. Journal of Cell Biology, 96(3), 717–721.

42. Kühn, U., & Pieler, T. (1996). Xenopus poly(A) binding protein: Functional domains in RNA binding and protein-protein interaction. Journal of Molecular Biology, 256(1), 20–30.

43. Gray, N. K., Coller, J. M., Dickson, K. S., & Wickens, M. (2000). Multiple portions of poly(A)-binding protein stimulate translation in vivo. Embo J, 19(17), 4723–4733.

44. Gallie, D. R. (1991). The cap and poly(A) tail function synergistically to regulate mRNA translational efficiency. Genes and Development, 5(11), 2108–2116.

45. Wakiyama, M., Imataka, H., & Sonenberg, N. (2000). Interaction of eIF4G with poly(A)-binding protein stimulates translation and is critical for Xenopus oocyte maturation. Current Biology, 10(18), 1147–1150.

46. Munroet, D., & Jacobson, A. (1990). mRNA Poly(A) Tail, a 3' Enhancer of Translational Initiation. Molecular and Cellular Biology, 10(7), 3441–3455.

47. Michel, Y. M., Poncet, D., Piron, M., Kean, K. M., & Borman, A. M. (2000). Cap-poly(A) synergy in mammalian cell-free extracts. Investigation of the requirements for poly(A)-mediated stimulation of translation initiation. Journal of Biological Chemistry, 275(41), 32268–32276.

48. Kahvejian, A., Roy, G., & Sonenberg, N. (2001). The mRNA closed-loop model: The function of PABP and PABP-interacting proteins in mRNA translation. Cold Spring Harbor Symposia on Quantitative Biology, 66, 293–300.

49. Gallie, D. R. (2014). Insights from a Paradigm Shift : How the Poly (A) -Binding Protein Brings Translating mRNAs Full Circle. New Journal of Science, 2014.

50. Borman, A. M. (2000). Biochemical characterisation of cap-poly(A) synergy in rabbit reticulocyte lysates: the eIF4G-PABP interaction increases the functional affinity of eIF4E for the capped mRNA 5'-end. Nucleic Acids Research, 28(21), 4068–4075.

51. Haghighat, A., & Sonenberg, N. (1997). eIF4g dramatically enhances the binding of eIF4E to the mRNA 5'-cap structure. *Journal of Biological Chemistry*, 272(35), 21677–21680.

52. Lee, K. a, Edery, I., & Sonenberg, N. (1985). Isolation and structural characterization of cap-binding proteins from poliovirus-infected HeLa cells. Journal of Virology, 54(2), 515–524.

53. Pelletier, J., & Sonenberg, N. (1985). Photochemical cross-linking of cap binding proteins to eucaryotic mRNAs: effect of mRNA 5' secondary structure. Molecular and Cellular Biology, 5(11), 3222–3230.
54. Borman, A. M., Michel, Y. M., Malnou, C. E., & Kean, K. M. (2002). Free poly(A) stimulates capped mRNA translation in vitro through the eIF4G-poly(A)-binding protein interaction. Journal of Biological Chemistry, 277(39), 36818–36824.

55. Von Der Haar, T., Oku, Y., Ptushkina, M., Moerke, N., Wagner, G., Gross, J. D., & McCarthy, J. E. G. (2006). Folding transitions during assembly of the eukaryotic mRNA cap-binding complex. Journal of Molecular Biology, 356(4), 982–992.

56. Gross, J. D., Moerke, N. J., Von Der Haar, T., Lugovskoy, A. A., Sachs, A. B., McCarthy, J. E. G., & Wagner, G. (2003). Ribosome loading onto the mRNA cap is driven by conformational coupling between eIF4G and eIF4E. Cell, 115(6), 739–750.

57. Okumura, F., Zou, W., & Zhang, D. E. (2007). ISG15 modification of the eIF4E cognate 4EHP enhances cap structure-binding activity of 4EHP. *Genes and Development*, 21(3), 255–260.